57：1－36（2012）

Inverse Modeling of Variably Saturated Subsurface Water Flow in Isothermal/Non-isothermal Soil

Tomoki IZUMI*

CONTENTS

Received March 15, 2012.
Accepted April 25, 2012.
*Lab. Water Resources Engineering

NOTATIONS

The following are the major symbols used in this thesis.

a_i = coefficient of piecewise cubic spline
a_i^k = coefficient of piecewise cubic spline
a_i^θ = coefficient of piecewise cubic spline
b_i = coefficient of piecewise cubic spline
b_i^k = coefficient of piecewise cubic spline
b_i^θ = coefficient of piecewise cubic spline
C_h = volumetric heat capacity
C_w = specific moisture capacity
c_i = coefficient of piecewise cubic spline
c_i^k = coefficient of piecewise cubic spline
c_i^θ = coefficient of piecewise cubic spline
c_s = volumetric heat capacity of soil particle
c_w = volumetric heat capacity of water
d_i = coefficient of piecewise cubic spline
d_i^k = coefficient of piecewise cubic spline
d_i^θ = coefficient of piecewise cubic spline
E = absolute error between observed and computed value
E^com = absolute error between observed and computed value with non-isothermal/free-form parameterization (FFP) model
E^iso = absolute error between observed and computed value with isothermal/FFP model
E^vg = absolute error between observed and computed value with non-isothermal/van Genuchten (VG) model
g = gravitational acceleration
$\boldsymbol{H}$ = Hessian matrix
h = hydraulic head
$\boldsymbol{I}$ = $I \times I$ unit matrix
J = total least squared error
K = unsaturated hydraulic conductivity
K_ad = admissible set of unknown parameter to be identified
K_r = relative hydraulic conductivity
$K_{\mathrm{r},i}(\cdot)$ = relative hydraulic conductivity function over the i th subdomain
$K_\mathrm{r}^\mathrm{FFP}(\cdot)$ = relative hydraulic conductivity function represented by FFP model
$K_\mathrm{r}^\mathrm{VG}(\cdot)$ = relative hydraulic conductivity function represented by van Genuchten-Mualem model
K_s = saturated hydraulic conductivity
K_T = temperature factor of hydraulic conductivity
$\boldsymbol{k}$ = vector of unknown parameter to be identified
$\boldsymbol{k}^\mathrm{opt}$ = vector of optimal parameter
k_i = value of $K_\mathrm{r}^\mathrm{FFP}$ at node i
L = total number of available observed data
m = number of iteration step
m_vg = parameter of VG model
n = number of time level
n_vg = parameter of VG model
P_ad = admissible set of $\boldsymbol{p}$
$\boldsymbol{p}$ = vector of unknown parameter to be identified
$\boldsymbol{p}^\mathrm{opt}$ = vector of optimal parameter

$\overline{q}$ = flux on Neumann boundary
q_h = heat flux
$\overline{q_h}$ = heat flux on Neumann boundary
q_w = water flux
$\overline{q_w}$ = water flux on Neumann boundary
R = rainfall
S_e = effective saturation
S_s = specific storage
S_w = saturation
T = time domain
T_0 = initial value of soil temperature
T_s = soil temperature
T_s^{com} = computed value of soil temperature
T_s^{obs} = observed value of soil temperature
T_s = soil temperature
$\overline{T_s}$ = value of T_s on Dirichlet boundary
t = time
w_l = weighting factor
z = independent variable for a vertical axis

Greek letters

α_{vg} = parameter of VG model
β_s = compressibility of soil
β_w = compressibility of water
Γ^D = Dirichlet boundary
Γ_h^D = Dirichlet boundary for heat transport
Γ_w^D = Dirichlet boundary for water movement
Γ^N = Neumann boundary
Γ_h^N = Neumann boundary for heat transport
Γ_w^N = Neumann boundary for water movement
γ = number of iteration
Δt = time step
ε = convergence criterion
η = control variable in terms of search direction
θ = volumetric water content
$\overline{\theta}$ = value of θ on Dirichlet boundary
$\boldsymbol{\theta}$ = vector of unknown parameter to be identified
$\theta^{FFP}(\psi)$ = soil water retention function represented with FFP model
$\theta^{VG}(\psi)$ = soil water retention function represented with VG model
θ^{com} = computed value of θ with non-isothermal/FFP model
θ^{iso} = computed value of θ with isothermal/FFP model
θ^{obs} = observed value of θ
θ^{vg} = computed value of θ with non-isothermal/VG model
θ_0 = initial condition of θ
θ_i = value of $\theta^{FFP}(\psi)$ at node i
$\theta_i(\psi)$ = soil water retention function over the ith subdomain
θ_r = residual water content
θ_s = saturated water content
$\varkappa$ = intrinsic permeability
λ = thermal conductivity
λ_0 = reference thermal conductivity
μ = dynamic viscosity
ρ = water density
ρ_r = water density at reference temperature
ρ_w = water density
ϕ = porosity
ψ = capillary head (on $\psi \leq 0$) or pressure head (on $\psi \geq 0$)
ψ_0 = initial value of ψ
$\overline{\psi}$ = boundary value of ψ on Dirichlet boundary
ψ^{com} = computed value of ψ with FFP model
ψ^{obs} = observed value of ψ
ψ^{vg} = computed value of ψ with VG model
Ω = space domain

LIST OF TABLES

LIST OF FIGURES

CHAPTER 1

INTRODUCTION

1.1 Background

1.1.1 Worldwide water crisis

The world is facing water crisis.

Water demand has been growing steadily in line with the population increase and economic growth with urbanization and industrialization. According to the United Nations Population Projections (medium variant of the 2010 version)[56], the world population stood at some 6.9 billion in 2010 and is expected to exceed 9.0 billion in 2050 and 10.0 billion by the end of this century. Though Cohen (1995)[7] estimated the maximum allowable world population as 7.0 billion based on the amount of renewable freshwater resources, in fact, water resources are running short because of the uneven distribution of renewable freshwater resources—in time and space. Using "Falkenmark indicator" or "water stress index" (Falkenmark, 1989[12]), people in the water stress state—when the per-capita maximum available amount of renewable freshwater resources falls below 1,700 cubic kilometers—are numbered approximately 0.7 billion in 2005 and 2.0 billion in 2008 (UNDP, 2006[55]; Ministry of the Environment, 2011[40]).

Furthermore, the climate change adds momentum to the water crisis. According to the Fourth Assessment Report (AR4) of the Intergovernmental Panel on Climate Change (IPCC)[24], the progress in global warming will expose several hundred million people to increased water stress in the coming years, and the increased frequency of droughts and flooding is projected to adversely impact food production. The rise in the global average temperature due to climate change is feared to bring about various impacts on water resources. The rapid urbanization is also noticeable and not only demand for domestic and industrial water is increased but also massive amounts of wastes and effluents are generated in association with mass consumption which aggravates the environmental load and deterioration of water quality (Ministry of the Environment, 2011[40]).

This crisis on both quality and quantity of water resources indicates that human activities have reached beyond the environmental carrying capacity. Thus, we, human beings are required to wisely and efficiently manage water resources based on the ideals of "sustainable development" propounded at the United Nations World Commission on Environment and Development in 1987.

1.1.2 Status of water use and multifunctionality of agriculture

Driven by solar energy and gravitational force, water globally circulates within the hydrosphere, the atmosphere, surface water, subsurface water and plants. From the global hydrologic cycle, human beings withdraw freshwater like surface and subsurface water for agriculture, industry and household with the ratio of 70%, 20% and 10%, respectively (FAO[13]). This tendency is closely the same in Japan (Ministry of Land, Infrastructure, Transport and Tourism, 2011[39]). Accordingly, it is impossible to sustainably plan or manage water use without considering agriculture, which is the largest withdrawing sector.

Agriculture plays the role of not only its primary function of food production but also the conservation of national lands, ecosystems and the environment through creating and maintaining a secondary nature. However, agriculture adversely impacts ecosystems, the global environment and even agricultural environment itself. The productivity-oriented agricide causes the reduction of soil and land fertility and leads to desertification. Application of large amount of pesticide and fertilizer diminishes water quality. Moreover, large scale irrigation in arid areas increases the problem of salt accumulation. It is, therefore, of great importance to quantitatively assess the effect of agricultural activities on the environment and to keep it below the threshold limit of sustainable range.

1.2 Research Aim and Objectives

This thesis aims at developing a methodology to identify the soil hydraulic properties with inverse technique to contribute to sophisticated numerical modeling of subsurface water flow phenomena that are basic and representative in irrigation agriculture. It is also quite useful to accurately estimate or predict subsurface water flow in substance transport problems dealing with the assessment of the influence of pesticide or fertilizer application and salt accumulation on water quality.

Generally, intensive and exhaustive investigations and analyses are required for the estimation of flow fields though it depends on the space scale of target area. To reduce labor and cost, numerical analyses have increasingly attracted lots of attention because of the great advances of computer technologies and capacities in recent years. The numerical analyses are required to reproduce a physical phenomenon of interest more accurately, and their success depends on the model structure given by the governing equations system and parameter identification which is a critical step in modeling process.

A physically-based mathematical model governing water flow in soil is represented by Richards equation (Richards, 1931[47]). Richards equation can be classified into three different forms based on the decision variables: a pressure-head-based (ψ-based) form, a moisture-content-based (θ-based) form, and a mixed form. According to Richards equation, the water movement through soil is derived from the gradient of hydraulic head under isothermal assumption, while water movement is also affected by soil temperature. It is, thus, necessary to deal with a coupling problem of water movement and thermal transport to represent of water movement near surface soil where heat energy exchange is quite significant.

On the other hand, it is also very important to identify model parameters included in the governing equations.

Model parameters in Richards equation are referred to as the soil hydraulic properties, *i.e.* the soil water retention curve and the unsaturated hydraulic conductivity. However, an identification method has not yet been established because these parameters are not directly measurable and have to be determined from historical observations.

Based on the above premises, the following proposals on inverse modeling of subsurface flow in isothermal and non-isothermal soil are the main objectives of this thesis:

(1) Inverse modeling for ψ-based form of Richards equation

(2) Inverse modeling for θ-based form of Richards equation

(3) Inverse modeling for mixed form of Richards equation

1.3 Structure of Thesis Framework

This thesis is organized into seven chapters including three original research papers of the author[26]−[28].

The introductory chapter gives an overview of the current status of water environment and discusses the importance of the water resources management in agriculture, which is the largest water withdrawing sector. The research aim and objectives are also presented, emphasizing the necessity of sophisticated subsurface water flow models to quantitatively assess the impacts of agriculture on the environment.

In Chapter 2, recent and pertinent studies on mathematical and numerical models for subsurface water flow in both isothermal and non-isothermal soil and representation and identification of model parameters—soil hydraulic properties—are reviewed.

In Chapter 3, an inverse modeling for ψ-based form of Richards equation in variably saturated and isothermal soil is proposed and discussed. To accurately describe subsurface water flow, the soil hydraulic properties, which is the unknown parameters to be identified, are represented by a free form parameterized function. As the parameterized function, a sequential piecewise cubic spline function is used in lieu of the conventional fixed form parameterized function. After an inverse problem is solved by simulation-optimization algorithm which combines a numerical model to solve a forward problem with a optimization method with the aid of the Levenberg-Marquardt method, the free form parameterized soil hydraulic properties are determined. The method developed is validated through twin experiments.

In Chapter 4, an inverse modeling for θ-based form of Richards equation in unsaturated and non-isothermal soil is proposed and discussed. Since water movement in surface soil is significantly affected by soil temperature, the forward problem on subsurface water flow is based on coupled water movement and heat transport equations. Validation of the method proposed is examined through applying to upland soil based on field observations using a proposed utilitarian observation system with simple instrumentation.

In Chapter 5, an inverse modeling for mixed form of Richards equation in variably saturated and isothermal soil is proposed and discussed. The success of numerical modeling depends on the model structure given by governing equations. Since the mixed form Richards equation is superior than the two other forms of Richards equation in terms of the range of application to saturation and conservation of mass balance, the forward problem in the inverse method is described as the mixed form Richards equation. The method is validated based on the same field observation in Chapter 4.

In Chapter 6, an inverse modeling for mixed form of Richards equation in variably saturated and non-isothermal soil is proposed and discussed. It is an extension of the method proposed in Chapter 5 to non-isothermal condition. The governing equation system is described as a coupled problem of mixed form Richards equation and heat conduction equation. From field observation, validation of the inverse method is carried out.

And, Chapter 7 presents the summary and conclusions of this thesis.

The matrix to illustrate the relation of the main chapters (Chapters 3 through 6) is shown in Figure 1.1.

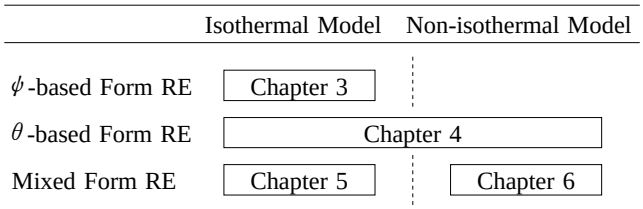

RE: Richards Equation

Figure 1.1: Structure of the main chapters

CHAPTER 2

LITERATURE REVIEW

2.1 Governing Equations for Subsurface Water Flow

2.1.1 Description of soil water movement and numerical method

Water movement in saturated porous media is described as the Darcy's law. The Darcy's law was improved by Buckingham in 1907 to present water flux in unsaturated porous media (Jury and Horton, 2004[30]). Additionally, the Darcy-Buckingham law has been extended by Richards (1931)[47] to transient flow, combined with the water conservation equation. Nowadays, the Richards equation is mostly used as the governing equation for subsurface water flow analysis.

Because of the highly nonlinear model parameters in Richards equation, analytical solutions are not generally possible except under very restricting assumptions regarding the parameters (Hillel, 1998[16]). Instead, various numerical methods such as the finite element method (FEM) have been developed and become a powerful technique with the advancement of computer technologies. Among those numerical methods, FEM is most frequently used because it enables us to analyze flow regions having complex geometric boundaries and arbitrary degrees of heterogeneity and anisotropy. FEM, which was first devised as a procedure for structural analysis, has been applied to steady and saturated seepage problems by Zienkiewicz (1966)[64]. Neuman and Witherspoon (1971)[45] have developed a finite element method to analyze unsteady flow with a free surface, extending the technique to solve steady state problems proposed by Neuman and Witherspoon (1970)[44]. Moreover, FEM has been applied to saturated-unsaturated flow analyses in porous media (Neuman, 1973[43]; Akai *et al*., 1977[1]).

From the view point of decision variables, Richards equation can be classified into following three forms:

(1) the ψ-based form,

(2) the θ-based form and

(3) the mixed form.

The ψ-based form of Richards equation has been most commonly used. This is because it can express all possible range of saturation where ψ is continuous. However, the disadvantage of ψ-based form is that it requires very fine spatial and temporal discretization to avoid computational instability and disproportionate mass balance since ψ is quite sensitive to change of θ in very dry conditions (Hills *et al*., 1989[17]). Various approaches have been proposed to overcome these disadvantages. Neuman (1973)[43] has proposed a mass lumping approach to improve numerical convergence and to eliminate numerical oscillations. Milly (1985)[38] has presented mass-conserving schemes that used a modified definition of the storage term to satisfy a global mass balance.

The θ-based form of Richards equation is derived by Klute (1952)[32]. The advantages of the form are that (1) water mass is automatically conserved within the computational domain regardless of time and spatial step size and (2) the hydraulic diffusivity—model parameter included in the θ-based form equation—does not vary with θ nearly as much as the unsaturated hydraulic conductivity varies with ψ. The disadvantage is that it cannot be used for simulating flow in soil near or at saturation since in that range the hydraulic diffusivity becomes infinite (Hillel, 1998[16]; Hills *et al*., 1989[17]).

The mixed form of Richards equation is an equation whose decision variables are both ψ and θ. Celia *et al*. (1990)[6] have presented a numerical model which pertains to the mixed form, perfectly conserving the mass using a modified Picard iteration method. After the work of Celia *et al*. (1990)[6], the mixed form has been used often as the governing equation for subsurface water flow, and the computational efficiency of its numerical model has improved (Huang *et al*., 1996[19]). Since almost all the numerical models proposed by Celia *et al*. (1990)[6] and subsequently others deal with only unsaturated zone, some extended models for saturated model as well as unsaturated model have been proposed (Takeuchi *et al*., 2008[54]; Zadeh, 2011[62]).

2.1.2 Water movement in non-isothermal soil

Richards equation expresses water movement through soil derived from the gradient of hydraulic head under isothermal condition while it is easily recognized that water movement is also forced by temperature gradient. When water movement near surface soil where heat energy exchange is quite significant is considered, coupled equation of water movement and heat transport is needed.

A theory on the simultaneous transfer of water and heat has formulated by Philip and de Vries (1957)[46] and de Vries (1958)[9] (PDV model). There have been various models based on PDV model. Kondo and Saigusa (1994)[33] had constructed a multi-layer soil model to estimate the evaporation from bare soil, incorporating a formula for vaporization in the soil pores in PDV model. On the other hand, Milly (1982)[36] has converted the equations of PDV model to the ψ-based formulation in order to extend the applicable range since PDV model is associated with the θ-based formulation. Milly model has been widely applied to the studies on evaporation from soil surface (Milly, 1984[37]), simultaneous transfer of water and heat in desert soil (Scanlon and Milly, 1994[48]), and so on. Moreover, Moukalled and Saleh (2006)[41] had proposed a numerical procedure to solve Milly model by the finite volume method being inherently conservative for the purpose of preventing the mass imbalance problem reported in the literature when employing the ψ-based formulation with other numerical methods.

Fujinawa (1995)[14] has presented a different formulation coupling water movement and heat transport. An equation derived from the generalized Darcy's law and the

Boussinesq assumption and an advection-dispersion equation are employed as governing equations for water movement and heat transport, respectively.

2.2 Soil Hydraulic Properties and Identification Method

To solve the basic equations governing subsurface water flow above mentioned, the soil hydraulic properties—the soil water retention curve (SWRC) and unsaturated hydraulic conductivity (UHC)—are needed. SWRC is defined as the relation between the volumetric water content and the matric suction, and UHC as a function of the saturation or suction.

2.2.1 Representation of soil hydraulic properties

The determination of UHC through laboratory or field measurement is generally laborious and time-consuming and, thus, it has been attempted to estimate UHC from SWRC which can be measured with relative ease. The representative models are Brooks and Corey (BC) model (Brooks and Corey, 1966[5]), van Genuchten-Mualem (VG) model (van Genuchten, 1980[59]; Mualem, 1976[42]) and Kosugi's lognormal pore-size distribution (LN) model (Kosugi, 1994[34]; 1996[35]). Among them, VG model is the most widely used for numerical analysis.

However, some drawbacks have been reported. According to Iden and Durner (2007)[21], although parameterizations of UHC coupled to SWRC by either empirical equations or capillary models are physically motivated, such approaches may give rise to practical problems, since (1) the capillary model itself may be only approximately valid for the porous medium under study and (2) any error of the employed model of SWRC propagates into errors in the predicted UHC. Additionally, Durner (1994)[10] has reported that the conventional unimodal retention function cannot describe SWRC in soil with heterogeneous pore systems, and proposed a flexible SWRC function formed by superimposing unimodal retention curve of VG model type. Moreover, Vogel *et al*. (2001)[61] have pointed out that the UHC derived from VG model can be quite sensitive to the shape of SWRC near saturation with unfavorable consequences for the computational performance in the numerical simulations, and presented a modified VG model. VG model could also lead to wrong predictions of UHC under the condition where air-entry effects are significant (Ippisch *et al*., 2006[25]).

Another alternative approach is a free-form parameterization approach (*e.g.* Kastanek and Nielsen, 2001[31]; Bitterlich *et al*., 2004[3]). The approach describes the soil hydraulic property with a sequential piecewise polynomial function. The function is referred to as "the free form function" in contrast with the function of conventional model like VG model being "the fixed form function". The advantages of the approach is that it offers high flexibility because of no *a priori* assumption about the specific shape of function and the number of parameters (Bitterlich *et al*., 2004[3]).

2.2.2 Identification method

The soil hydraulic properties are determined by direct measurement or indirect method. The direct measurement methods are summarized by Japanese Association of Groundwater Hydrology (2010)[29]. Though the direct measurement of SWRC is possible with wide range of pressure head, the direct measurement of UHC is difficult because it is laborious and time-consuming (Hillel, 1998[16]).

Accordingly, the indirect method—inverse method—has been focused on because of the advantage of optimization techniques and computer power. The inverse method is based on two methodologies: (a) the multistep outflow method (Eching and Hopmans, 1993[11]; van Dam *et al*., 1994[58]) and (b) the evaporation method (Šimůnek *et al*., 1998[57]).

Bitterlich *et al*. (2004)[3] have proposed an inverse method to estimate the soil hydraulic properties using free form functions through column outflow experiments. Iden and Durner (2007, 2008)[21],[22] have estimated the soil hydraulic properties in the similar framework of inverse modeling to the work of Bitterlich (2004)[3], based on the multistep outflow method and evaporation method, respectively.

Zhang *et al*. (2010)[63] have presented an inverse method based on field experiments. In their method, FAO approach (Allen *et al*., 1998)[2] is embedded to calculate the potential evapotranspiration in the forward solution procedure, since measurement of actual evapotranspiration is generally difficult in field experiments.

CHAPTER 3

INVERSE METHOD TO IDENTIFY SOIL HYDRAULIC PROPERTIES IN VARIABLY SATURATED SUBSURFACE WATER FLOW MODEL —ψ-BASED FORM OF RICHARDS EQUATION—

3.1 Introduction

The methodical way to numerically model and reproduce a real groundwater system is at the outset to solve an inverse problem (IP) to estimate *a priori* unknown parameters included in the groundwater equations system, and subsequently to solve a forward problem (FP) for obtaining solutions to the equations with the parameters so estimated. A variety of well-developed methods to solve FPs are currently available (*e.g.*, Huyakorn and Pinder, 1983[20]). Since reliability of the solutions to FP is contingent on the model parameters to be estimated prior to these solutions, development of the performance solver for IP is also an essential need.

Here, inverse modeling for Richards equation which is a standard mathematical model for saturated-unsaturated groundwater flow in a porous medium is considered. Conventionally, soil hydraulic properties (*i.e.*, the relative hydraulic conductivity K_r and the volumetric water content θ), which are major parameters in the equation, are described by the fixed-form functions expressed in terms of the unknown variable (*i.e.*, the pressure head ψ), which cover a possible global range of the variable. Most of the earlier works on the solution of IP are based on the flow model with this type of parameterization in a fixed functional form. For instance, Hsu and Liu (1990)[18], and Constales and Kačur (2001)[8] proposed the methods to identify a set of the functions which consists of the closed-form equations by van Genuchten (1980)[59], called VG model. Takeshita and Kohno (1993)[52] attempted to identify the soil water retention curve relating θ with ψ, based on the VG model. Si and Kachanoski (2000)[50] proposed a method of the solution of IP based on another fixed functional model by Broadbridge and White (1988)[4]. Solution of IP based on this parameterization is indeed less laborious since the number of the parameters to be estimated is limited. However, drawbacks arise from less flexibility or small degree of freedom due to the specific shape of the functions. There is every possibility that assumptions made for formulating the functions (*e.g.*, assumed pore-size distribution) are invalid for the actual soil hydraulic properties of interest. In use of the VG model that is most commonly used, the conductivities derived from this model can be quite sensitive to the shape of the soil water retention curve near saturation with unfavorable consequences for the computational performance in the solution of FP (Vogel *et al*., 2001[61]). Under particular conditions where effects of the air-entry are significant, the VG model could lead to wrong predictions of the conductivities (Ippisch *et al*., 2006[25]).

As an alternative inverse modeling approach to overcome these drawbacks, Bitterich *et al*. (2004)[3] used the free-form parameterization in which particular polynomial functions were employed to describe the soil hydraulic properties within a small partitioned range of the entire pressure head domain, and in principle the number of parameters—the number of degrees of freedom—could freely be selected. Two different polynomial functions (quadratic B-splines and piecewise cubic Hermite interpolation), expressed in terms of the pressure head, were employed to comparatively investigate their performances in the solution of IP. The validity of the proposed approach was examined based on the data from the outflow experiments for soil columns. Using a sequential programming method, the functions best at fitting the soil hydraulic properties were identified through minimizing the objective function which was defined as a weighted sum of the squared errors between measured (experimental) and numerically calculated outflow rates from the bottom of the soil column. However, no detailed algorithm for parameter optimization was presented.

This chapter is associated with development of a field-oriented approach for the inverse estimation of the soil hydraulic properties which is based on the free-form parameterization. Assuming the properties are dominantly one-dimensional and independent of thermal transport in the soil, *i.e.*, considering an isothermal soil water movement in a column, a methodology for parameter estimation is developed and validated which would be advantageous to the solution of IP. By assembly of the piecewise cubic spline functions, each of K_r and θ is expressed as a continuous function of the pressure head. To find the shapes of such functions best expressing head-dependency of the soil hydraulic properties, a simulation-optimization algorithm with the aid of the Levenberg-Marquardt method is developed which serves to iteratively solve an optimization problem of minimizing errors between the observed and computed values of the pressure head in combination with the embedded simulation module for forward solutions. The term *"field-oriented"* is used to indicate that the errors are measured in terms of the head rather than the outflow rate which is difficult to be *in-situ* observed, and therefore solution of the IP can be achieved having only recourse to the observed time-series data of pressure head.

3.2 Forward Problem

The governing equation of one-dimensional saturated-unsaturated groundwater flow is expressed by the Richards equation as follows.

$$(C_w + S_s)\frac{\partial \psi}{\partial t} = -\frac{\partial}{\partial z}\left(-K(\psi)\frac{\partial h}{\partial z}\right) \tag{3.1}$$

where C_w is the specific moisture capacity, S_s the specific storage, $\psi(z,t)$ the capillary head (on $\psi < 0$) or pressure head (on $\psi \geq 0$), $h(z,t)$ the hydraulic head ($h = z + \psi$), $K(\psi)$ unsaturated hydraulic conductivity, z the height defined as positive upward from the bottom of the soil and t the time.

The specific moisture capacity C_w, the specific storage S_s and the unsaturated hydraulic conductivity $K(\psi)$ are defined as follows.

$$C_w(\psi) = \begin{cases} \dfrac{d\theta}{d\psi} & (\psi < 0) \\ 0 & (\psi \geq 0) \end{cases} \tag{3.2}$$

$$S_s(\psi) = \rho g \left(\beta_s \frac{\theta}{\theta_s} + \theta \beta_w \right) \tag{3.3}$$

$$K(\psi) = \begin{cases} K_s K_r(\psi) & (\psi < 0) \\ K_s & (\psi \geq 0) \end{cases} \tag{3.4}$$

where K_s is the saturated hydraulic conductivity, $K_r(\psi)$ the relative hydraulic conductivity, θ the volumetric water content, ρ the water density, g the gravitational acceleration, β_w the coefficient of water compressibility and β_s the coefficient of soil compressibility.

Eq.(3.1) is considered subject to the following initial and boundary conditions with the given or specified values of ψ_0, $\overline{\psi}$ (on Dirichlet boundary Γ^D) and $\overline{q}$ (flux on Neumann boundary Γ^N).

$$\psi(z, 0) = \psi_0 \quad \text{in} \quad \Omega \tag{3.5}$$

$$\psi(z, t) = \overline{\psi} \quad \text{on} \quad \Gamma^D \times T \tag{3.6}$$

$$-K_s K_r \frac{\partial h}{\partial z} = \overline{q} \quad \text{on} \quad \Gamma^N \times T \tag{3.7}$$

Given that the coefficients of the derivatives in Eq.(3.1) are well parameterized or related to the unknown variable ψ, it can be numerically solved with respect to ψ by a combined use of the standard Galerkin finite element method and the implicit time-marching scheme (Crank-Nicolson scheme) which provides unconditionally stable solutions. This forward solution model is embedded in the parameter optimization process described below, and serves to simulate the flow for the soil hydraulic properties stepwise updated in the process.

3.3 Inverse Problem

3.3.1 Parameterization

For free-form parameterization, the individual relations must be expressed by functions which are continuously differentiable over the whole domain of interest. For this purpose, as shown in Figure 3.1, the whole domain is partitioned into (I-1) subdomains with I nodes (I denotes the degrees of freedom of the parameterization), and each of the functions for K_r and θ over the whole domain is expressed by an assembly of piecewise cubic spline interpolation functions each of which is locally defined over a confined subdomain bounded with two nodes. Thus, the functions defined over i-th subdomain of $[\psi_i, \psi_{i+1})$ $(\psi_i < \psi_{i+1})$, $K_{r,i}(\psi)$ and $\theta_i(\psi)$ are described as follows.

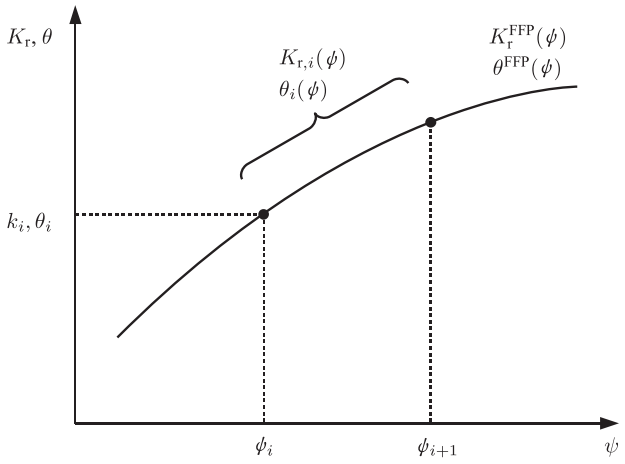

Figure 3.1: Cubic splines

$$K_{r,i}(\psi) = \begin{cases} a_i^k + b_i^k(\psi - \psi_i) + c_i^k(\psi - \psi_i)^2 \\ \quad + d_i^k(\psi - \psi_i)^3 & \text{in} \quad [\psi_i, \psi_{i+1}) \\ 0 & \text{otherwise} \end{cases} \tag{3.8}$$

$$\theta_i(\psi) = \begin{cases} a_i^\theta + b_i^\theta(\psi - \psi_i) + c_i^\theta(\psi - \psi_i)^2 \\ \quad + d_i^\theta(\psi - \psi_i)^3 & \text{in} \quad [\psi_i, \psi_{i+1}) \\ 0 & \text{otherwise} \end{cases} \tag{3.9}$$

where a_i^k, b_i^k, c_i^k, d_i^k, a_i^θ, b_i^θ, c_i^θ and d_i^θ are the coefficients in the cubic splines and i $(1 \leq i \leq I)$ nodal number. The shapes of the functions to be determined are therefore expressed as an assembly of the local functions so defined.

$$K_r^{FFP}(\psi) = \sum_i K_{r,i}(\psi) \tag{3.10}$$

$$\theta^{FFP}(\psi) = \sum_i \theta_i(\psi) \tag{3.11}$$

Hereinafter, the values of $K_r^{FFP}(\psi_i)$ and $\theta^{FFP}(\psi_i)$ at the node i are simply denoted by k_i and θ_i, and their sets by $\boldsymbol{k}$ and $\boldsymbol{\theta}$, respectively. Since, as well known, the soil hydraulic properties monotonously increase with the increasing head, Eqs.(3.10) and (3.11) must be identified so that the following constraints are satisfied.

$$k_i \leq k_{i+1}, \quad \theta_i \leq \theta_{i+1} \tag{3.12}$$

3.3.2 Solution procedure of IP

At first, a set of decision variables $\boldsymbol{p}$ is defined to represent both the unknown parameter sets $\boldsymbol{k}$ and $\boldsymbol{\theta}$.

$$\boldsymbol{p} = \begin{cases} p_m = k_m & (m = 1, \cdots, I) \\ p_m = \theta_{m-I} & (m = I+1, \cdots, 2I) \end{cases} \tag{3.13}$$

Searching for the sets of the optimal solutions, $\boldsymbol{p}^{opt}$, is then achievable through minimizing the objective function, defined as the total squares error integrated over space and time between the solution of FP ($\psi^{com}(\boldsymbol{p})$) and the observation data (ψ^{obs}), and therefore written as

$$J(\boldsymbol{p}^{\text{opt}}) = \min J(\boldsymbol{p}),\ \boldsymbol{p}^{\text{opt}},\ \boldsymbol{p} \in P_{\text{ad}} \tag{3.14}$$

with

$$J(\boldsymbol{p}) = \frac{1}{2}\sum_{l=1}^{L}\{f_l(\boldsymbol{p})\}^2 \tag{3.15}$$

$$f_l(\boldsymbol{p}) = \phi_l^{\text{com}}(\boldsymbol{p}) - \phi_l^{\text{obs}} \tag{3.16}$$

where P_{ad} is the admissible sets of $\boldsymbol{p}$ and L the total number of observation data available in the space $\Omega \times \mathrm{T}$.

In the process of minimizing Eq.(3.14) subject to Eq. (3.12), the decision variables $\boldsymbol{p}$ are iteratively updated while step by step solving FP with their assumed or previously estimated values. In this respect, identification of the functions (Eqs.(3.10) and (3.11)) requires a sort of simulation-optimization technique. The entire procedure for solving IP is illustrated in Figure 3.2.

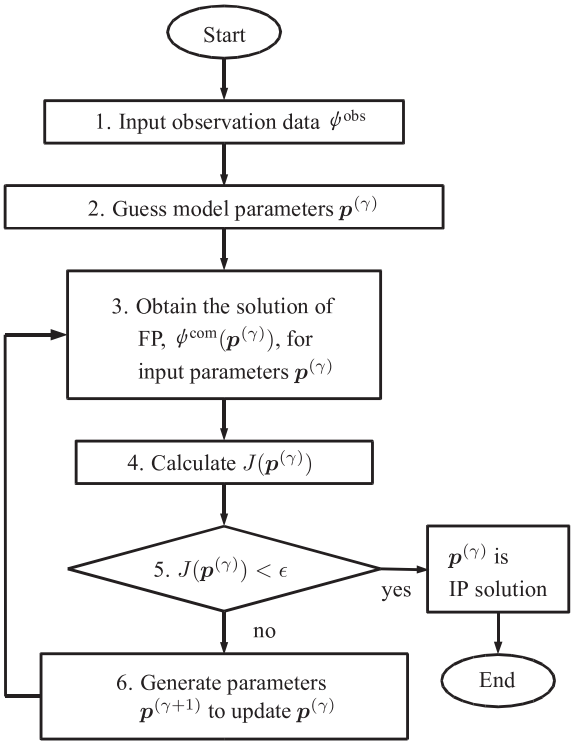

Figure 3.2: Solution search algorithm

3.3.3 Optimization algorithm

Levenberg-Marquardt method, which is a modified Gauss-Newton method, is adopted for the optimization algorithm. With this method, the unknown parameters are step by step updated with the following search sequence through the iteration.

$$\boldsymbol{p}^{(\gamma+1)} = \boldsymbol{p}^{(\gamma)} + \Delta\boldsymbol{p}^{(\gamma)} \tag{3.17}$$

with

$$\Delta\boldsymbol{p}^{\gamma} = -(\boldsymbol{H}^{(\gamma)} + \eta\boldsymbol{I})^{-1}\nabla J^{(\gamma)} \tag{3.18}$$

$$\boldsymbol{H}^{(\gamma)} = \left[\sum_{l=1}^{L}\frac{\partial f_l^{(\gamma)}}{\partial p_i}\frac{\partial f_l^{(\gamma)}}{\partial p_j}\right] \tag{3.19}$$

where γ is the iteration number, η a coefficient and $\boldsymbol{I}$ a $(2I)\times(2I)$ unit matrix. When η is equal to 0, $\Delta\boldsymbol{p}^{(\gamma)}$ reduces to the Gauss-Newton direction. On the other hand, when η tends to infinity, $\Delta\boldsymbol{p}^{(\gamma)}$ turns to the steepest descent direction and size of $\Delta\boldsymbol{p}^{(\gamma)}$ tends to zero. Therefore, η is taken as 0 for an initial value, and if $J(\boldsymbol{p}^{(\gamma+1)}) < (\boldsymbol{p}^{(\gamma)})$ is not satisfied, then value of η is increased and $\Delta\boldsymbol{p}^{(\gamma)}$ is recomputed with Eq.(3.17) until the reduction condition $J(\boldsymbol{p}^{(\gamma+1)}) < J(\boldsymbol{p}^{(\gamma)})$ is satisfied (Sun, 1994[51]).

3.4 Validation

3.4.1 Methods

The validity of the methodology presently developed is primarily examined with its application to a hypothetical soil column as shown in Figure 3.3. The column of 30 cm high is assumed to be homogeneous, and bounded on its bottom end by fully saturated groundwater. For the forward solution which is needed in solution search sequence for parameter optimization, the spatial domain being considered is discritized into 6 line-elements of equal length with 7 nodes.

Observation of the pressure head is assumed to be made at three different locations depicted by the black square dots in Figure 3.3. Since actual observation data from measurements are unavailable, substitutes for them are numerically generated. For this, the forward problem is solved with the same spatial discretization as in Figure 3.3, assuming that the soil hydraulic properties could be well represented by the VG model written as

$$K_{\text{r}}^{\text{VG}}(\psi) = (S_{\text{e}})^{\frac{1}{2}}\left(1-\left(1-(S_{\text{e}})^{\frac{1}{m_{\text{vg}}}}\right)^{m_{\text{vg}}}\right)^2 \tag{3.20}$$

$$S_{\text{e}}(\psi) = \frac{\theta-\theta_{\text{r}}}{\theta_{\text{s}}-\theta_{\text{r}}} = \frac{1}{(1+(\alpha_{\text{vg}}|\psi|)^{n_{\text{vg}}})^{m_{\text{vg}}}} \tag{3.21}$$

$$\theta^{\text{VG}}(\psi) = \theta_{\text{r}} + \frac{\theta_{\text{s}}-\theta_{\text{r}}}{(1+(\alpha_{\text{vg}}|\psi|)^{n_{\text{vg}}})^{m_{\text{vg}}}} \tag{3.22}$$

where S_{e} is the effective saturation estimated by the VG model, θ_{s} the saturated water content, θ_{r} the residual water content, α_{vg}, m_{vg} and n_{vg} parameters that shape the soil properties and have relation as $m_{\text{vg}} = 1 - 1/n_{\text{vg}}$.

Considering a one-way process of desorption, the whole domain of interest is assumed to be initially saturated, and unsaturated due to quick drainage of the water absorbed in soils, *i.e.*, due to quick fall of the phreatic surface from the top to the bottom of the column. This means that the soil hydraulic properties under a condition repeating wet and dry, *i.e.*, affected by hysteresis, are not considered. In addition, $\overline{\psi} = 0$ cm and $\overline{q} = 0$ cm/s are given to the bottom and top boundaries of the column, respectively. Specification of no-flow through the top boundary is correct in reality because the desorption process could be completed during a so short period of time that effects of rainfall and/or evaporation can be neglected.

For comparative examinations, two different soil types (Soil A and Soil B) with different soil hydraulic properties are considered which are characterized by less and more sensitive changes of the relative hydraulic

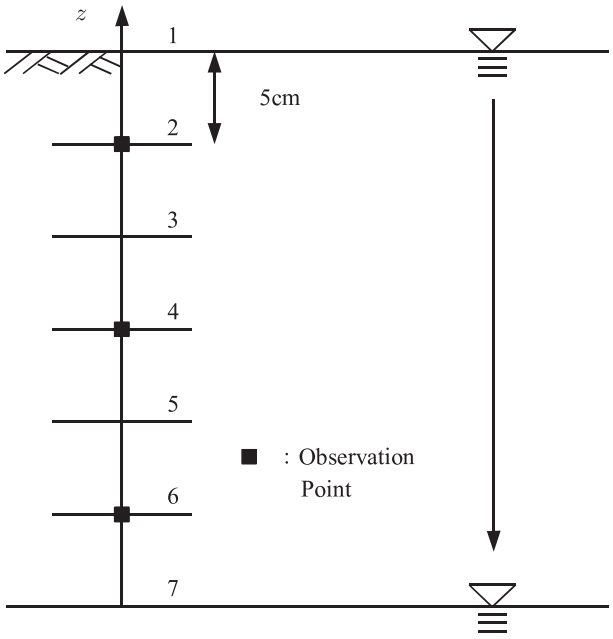

Figure 3.3: Soil column

conductivity near saturation, respectively. Soil A and Soil B are those like volcanic ash soil (*andosol*) and subsoil of the volcanic ash soil (loamy soil), respectively. Values of the parameters to be specified for simulation runs to generate observation data as well as for simulation-optimization runs are summarized in Table 3.1 for those common for both soils, Tables 3.2 and 3.3 for Soil A and Soil B, respectively.

In order to generate observation data for this desorption process, it is enough in any case to simulate the flow over a period of 5 minutes during which the flow certainly falls steady—timeindependent. For solving this forward problem, the time is marched with the relatively small increment of 0.1 s to reproduce the time-varying flow in the column at high resolution. All of the time-dependent discrete solutions of pressure head, obtained at selected three observation points, are employed as observation data as they are. This indicates that the generated pseudo observation data are spatially selected part of the true solutions to the flow problem under consideration, and therefore the observation is made at intervals of 0.1 s having no measurement errors and noises.

Taking into account the abovementioned characteristics of the individual soils, the entire domain of the pressure head is partitioned at even intervals into 6 subdomains for Soil A, and more finely, 10 subdomains for Soil B to find the function with better fitness to the relative hydraulic conductivity which is quite sensitive near saturation.

3.4.2 Results

Figures 3.4 and 3.5 illustrate the identified functions of the relative hydraulic conductivity and the volumetric water content, $K_r^{FFP}(\psi)$ and $\theta^{FFP}(\psi)$, for Soil A in comparison with the true functions, $K_r^{VG}(\psi)$ and $\theta^{VG}(\psi)$, based on the VG model, respectively. Figure 3.6 shows the timevarying pressure heads at three selected

Table 3.1: Common parameters

Parameter	Value
β_s [cm^2/N]	2.0×10^{-4}
β_w [cm^2/N]	4.4×10^{-6}
k_{up}	1.0
k_{low}	0.0
θ_{up}	θ_s
θ_{low}	θ_r

Table 3.2: Parameters of Soil A

Parameter	Value
θ_s	0.801
θ_r	0.581
K_s [cm/s]	7.0×10^{-4}
VG model parameter	
α_{vg} [cm^{-1}]	0.0268
n_{vg}	3.249

Table 3.3: Parameters of Soil B

Parameter	Value
θ_s	0.760
θ_r	0.218
K_s [cm/s]	4.5×10^{-3}
VG model parameter	
α_{vg} [cm^{-1}]	0.0115
n_{vg}	1.487

locations—of major concern in practical respects—for the same soil type, which are part of the solutions obtained from simulation practice with the identified functions for the soil hydraulic properties, including those from pseudo observation—true heads. Figure 3.7 illustrates the variations of the absolute error $|\psi^{com}-\psi^{obs}|$ of those computed pressure heads from the observed (true) ones, which helps closely investigating reproducibility (accuracy) of the solutions resulting from using the identified functions. Correspondingly, the results for Soil B are shown in the insert of Figures 3.8 through 3.11.

Function identifiability for Soil A is so high that indistinguishable discrepancies between $K_r^{FFP}(\psi)$ and $K_r^{VG}(\psi)$ as well as between $\theta^{FFP}(\psi)$ and $\theta^{VG}(\psi)$ can be found over the entire domain of pressure head (Figures 3.4 and 3.5). The function of relative hydraulic conductivity for Soil B is, however, perceptibly discrepant within the limited range of the head near saturation, though the function of volumetric water content is identified favorably with its true one (Figures 3.8 and 3.9). This partially discrepant proneness in identification of the conductivity function could be eliminated by augmenting the number of subdomains for the corresponding range. The forward solutions resulting from using the duly identified functions for the soil hydraulic properties are satisfactory with good agreement to the true

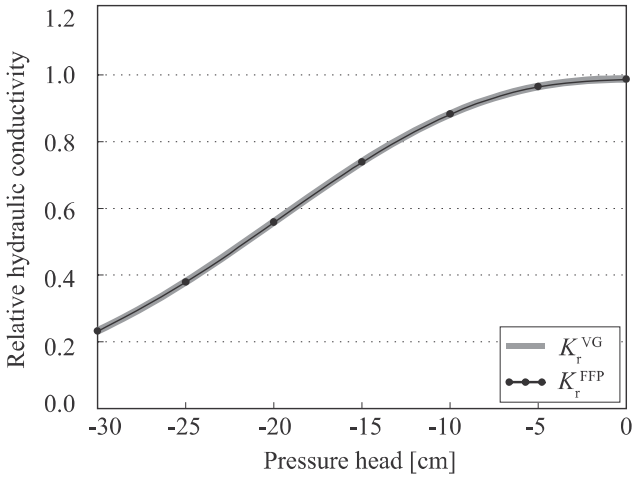

Figure 3.4: K_r^{FFP} compared with K_r^{VG} (Soil A)

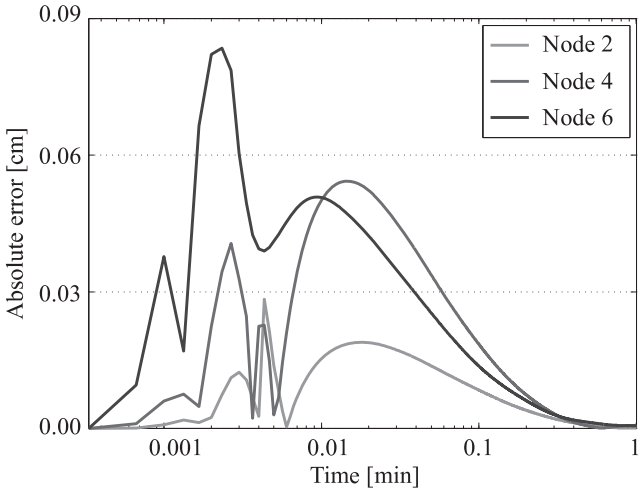

Figure 3.7: Absolute errors between computed and true pressure heads (Soil A)

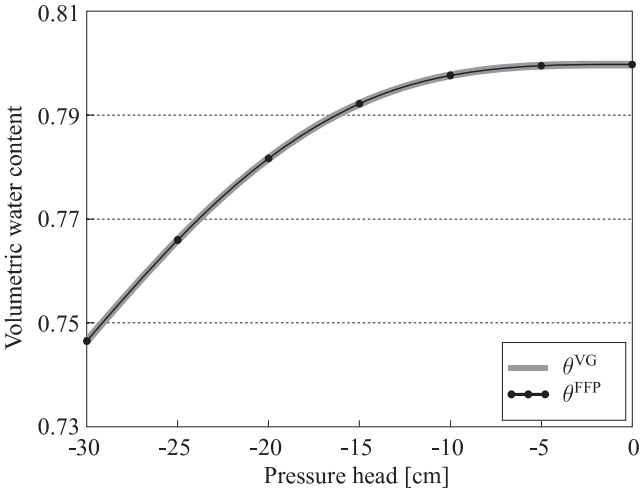

Figure 3.5: θ^{FFP} compared with θ^{VG} (Soil A)

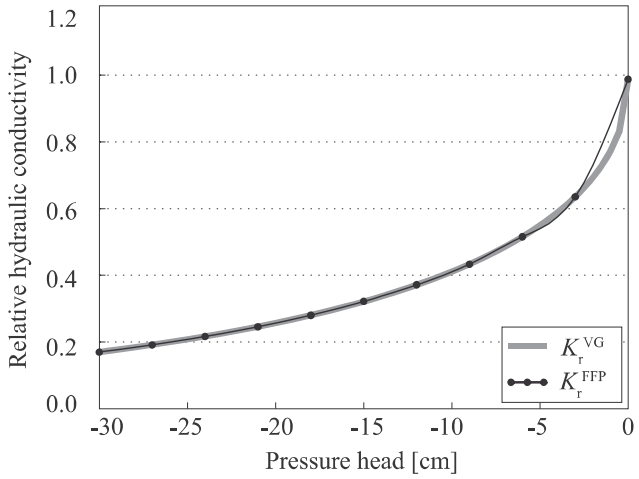

Figure 3.8: K_r^{FFP} compared with K_r^{VG} (Soil B)

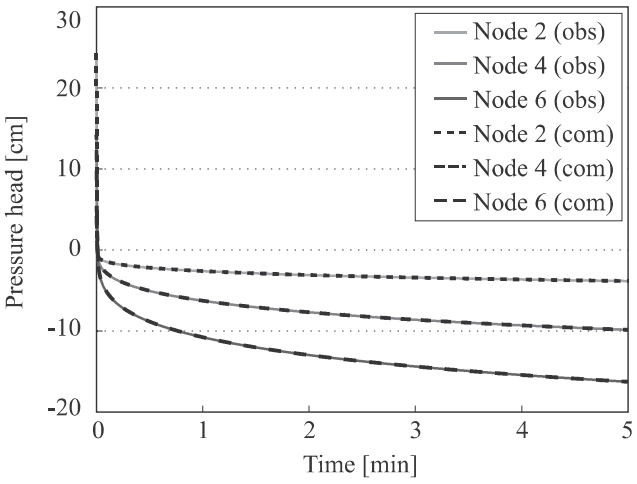

Figure 3.6: Time-varying pressure heads (Soil A)

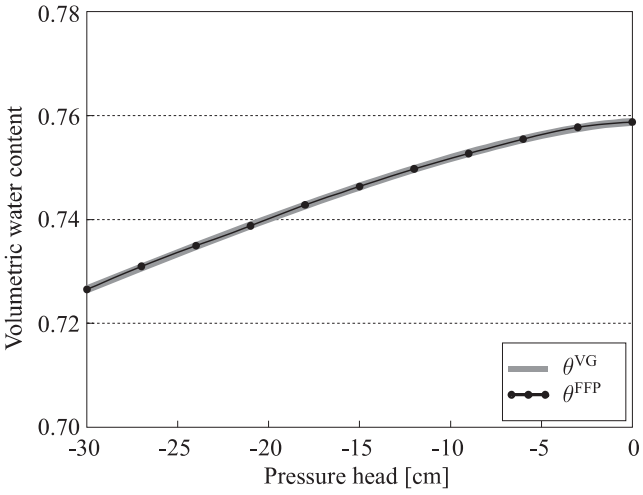

Figure 3.9: θ^{FFP} compared with θ^{VG} (Soil B)

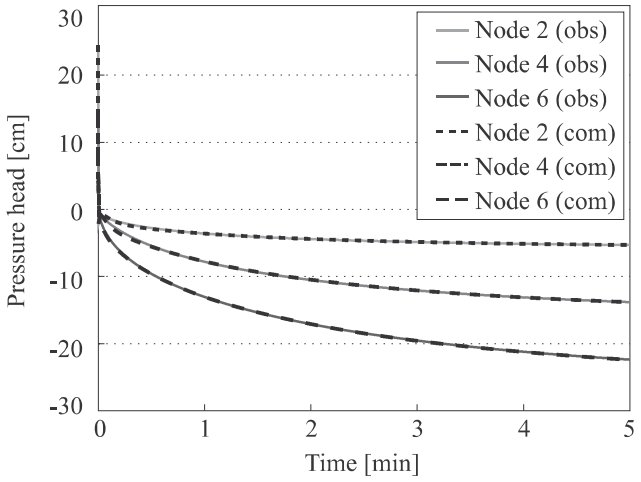

Figure 3.10: Time-varying pressure heads (Soil B)

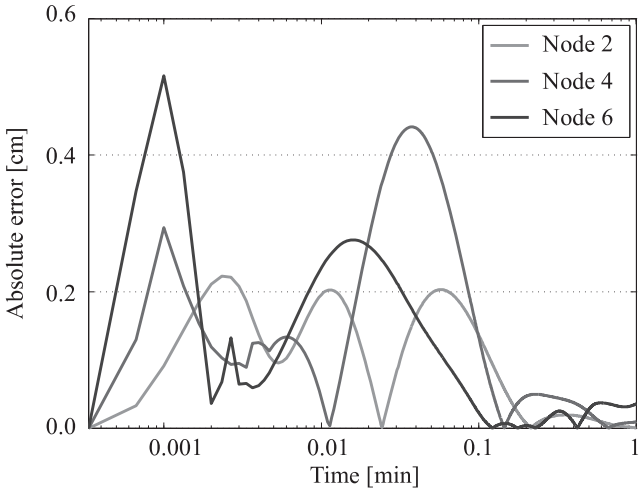

Figure 3.11: Absolute errors between computed and true pressure heads (Soil B)

solutions (Figures 3.6 and 3.10). Perceptible deviation from the true solutions—at most 1 mm and 5 mm for Soil A and Soil B, respectively—occurs during a short period of time just after the quick commencement of dewatering from the column, and dwindles away as time passes (Figures 3.7 and 3.11).

The results shown above prove that the present inverse method enables us to well estimate the soil hydraulic properties in a functional form, yielding unique and stable inverse solutions even in a case of unrealistic discontinuous flow dynamics like quick desorption.

3.5 Conclusions

In this chapter, an approach for identifying in a functional form the unknown quantities—soil hydraulic properties—parameterized in saturated-unsaturated groundwater flow model has been developed. The individual soil hydraulic properties are interpolated by piecewise cubic spline functions in a relation between the property and the pressure head. The inverse problems defined are solved as the problems of determining the coefficients of the functions in a framework of the simulation-optimization. Requiring field observations of the time-varying pressure head alone, the approach is field-oriented, and therefore less costs us to solve the problems. The approach has been proved to be valid through its practical application to a hypothetical soil column, identifying the parameters with well-performance. This suggests that the approach developed could be a viable alternative to the conventional fixed functional form approaches.

CHAPTER 4

INVERSE METHOD TO IDENTIFY UNSATURATED HYDRAULIC CONDUCTIVITY IN VARIABLY SATURATED SUBSURFACE WATER FLOW MODEL IN NON-ISOTHERMAL SOIL —θ-BASED FORM OF RICHARDS EQUATION—

4.1 Introduction

Because of increasing demand for numerical analysis and importance of parameter identification being key to success the analysis, Takeuchi *et al*. (2007)[53] and Izumi *et al*. (2008)[28] proposed an inverse method with the free-form parameterization to estimate soil hydraulic properties only from the observed time-series field data, and verified its effectiveness through numerical tests considering different combinations of the degree of freedom in the parameterization, logging interval and observation error.

Izumi *et al*. (2008)[28] was based on the governing equation under isothermal assumption. The method developed is, therefore, unsuited for the non-isothermal situation where due to active heat energy exchange through a soil surface the soil temperature distribution becomes so non-uniform that it significantly affects water movement. Generally, it is known that the soil temperature influences the surface tension and viscosity of water. From the field observation conducted by the author, in fact, it is claimed that the temperature dependency of the surface tension leads to a change in the water flux, estimated by the formula in Kondo and Saigusa (1994)[33], at the rate of a few percent, while the temperature dependency of the viscosity to a change in the saturated hydraulic conductivity at the rate of about 40% in the changeable range of soil temperature. Also, Inoue *et al*. (2004)[23] showed that the air temperature influenced readings of tensiometer, from the distinct differences between the suction values observed in daytime and nighttime at the same water content.

In this chapter, an extension of the previous work (Izumi *et al*., 2008[28]) to develop a general inverse method applicable even for a non-isothermal seepage or subsurface flow is presented. First, an *in-situ* observation system with simple instrumentation is presented which implements collection of the hydro-geological data—volumetric water content, suction and soil temperature—necessary for solving IP. After definition of FP, solution procedure for the inverse problem in that the relative hydraulic conductivity (RHC) is identified by use of the free-form parameterization technique is described, and validity of the inverse method developed is examined through its application to the soil of a real upland crop field, or through calibration tests of the coupled water movement and thermal conduction models, for the desorption process in that considering the hysteretic phenomenon is not needed. In addition, efficacy of allowing for soil temperature variability—non-isothermal condition—in the forward problem is verified.

4.2 Method

4.2.1 Observation system

A typical observation system for acquiring the necessary data at a few different depths in a soil column is shown in Figure 4.1. A set of three soil moisture probes, one tensiometer and two thermometers, which are drawn by black lines or painted black, is a basic instrumentation or a minimum requirement for the purpose of the observation. The remaining instruments, depicted in gray, are optional. Two or three different instruments should be paired and aligned in the same depth.

The data of basic need, obtained from the basic instrumentation, are put to use as follows. The volumetric water contents and the soil temperatures at both top and bottom ends of a soil column, observed by the soil moisture probes and the thermometers, respectively, are used as Dirichlet boundary values for the governing equations to solve a FP. The volumetric water content observed by the intermediate soil moisture probe is used to evaluate the fitness of an unsaturated hydraulic conductivity function—actually a relative hydraulic conductivity function—in an optimization process. A pair of volumetric water content and suction data in the same depth is used to identify a soil water retention property.

Supplement of one or two optional tensiometers serves to improve reliability of the soil water retention property. An additional thermometer in the intermediate depth provides the benchmark data for verifying reproducibility of forward solution.

The system is extremely simple. Thus, it is inexpensive and can be buried in the ground without spending time and effort, less disturbing the soil column of interest.

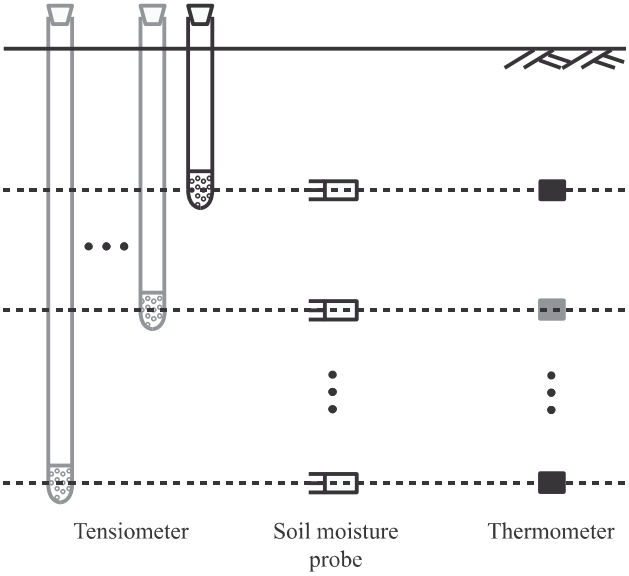

Figure 4.1: Basic and optimal instruments for field observations

4.2.2 Forward problem

Assumed to be predominantly one-dimensional, the seepage flow in variably saturated and nonisothermal soil can be described by coupled water mass (water movement) and energy balance (thermal conduction) equations (Kondo and Saigusa, 1994[33]). The mass balance allowing for effects of soil temperature in soil, neglecting vapor fluxes, is represented in terms of volumetric water content as follows.

$$\rho_w \frac{\partial \theta}{\partial t} = -\frac{\partial q_w}{\partial z} \tag{4.1}$$

with

$$q_w = -\rho_w D_\theta \frac{\partial \theta}{\partial z} - \rho_w D_T \frac{\partial T_s}{\partial z} - \rho_w K \tag{4.2}$$

$$D_\theta = K \frac{\partial \psi}{\partial \theta} = \frac{K}{C_w} \tag{4.3}$$

$$D_T = K \frac{\partial \psi}{\partial T_s} \tag{4.4}$$

$$K = K_r K_s \tag{4.5}$$

$$K_s = \frac{\varkappa}{\mu(T_s)} \rho_w g \tag{4.6}$$

where ρ_w is the water density and assumed to be constant here, θ the volumetric water content, t the time, z the height defined as positive upward, T_s the soil temperature, ψ the suction, C_w the specific moisture capacity, K the unsaturated hydraulic conductivity, K_r the relative hydraulic conductivity, K_s the saturated hydraulic conductivity, $\varkappa$ the intrinsic permeability, μ the viscosity coefficient and g the gravitational acceleration.

The energy balance equation assuming a local thermal equilibrium between soil and water, to be coupled with Eq.(4.1), is described as follows.

$$C_h \frac{\partial T_s}{\partial t} = \frac{\partial q_h}{\partial z} \tag{4.7}$$

with

$$C_h(\theta) = (1-\theta_s) c_s + \theta c_w \tag{4.8}$$

$$q_h = -\lambda \frac{\partial T_s}{\partial z} \tag{4.9}$$

$$\lambda = \lambda_0 + 0.5\theta^{\frac{1}{3}} \tag{4.10}$$

where C_h is the volumetric heat capacity of soil, θ_s the saturated water content, c_s and c_w the volumetric heat capacity of soil particles (1.26×10^6 [J/(m^3·K)]) and that of water (4.20×10^6 [J/(m^3·K)]), respectively and λ the thermal conductivity of soil which is expressed in terms of the reference thermal conductivity λ_0.

Eqns.(4.1) and (4.7) are considered subject to the following initial and boundary conditions.

$$\theta(z,0) = \theta_0(z) \quad \text{in} \quad \Omega \tag{4.11}$$

$$T_s(z,0) = T_0(z) \quad \text{in} \quad \Omega \tag{4.12}$$

$$\theta(z,t) = \overline{\theta}(z,t) \quad \text{on} \quad \Gamma_w^D \tag{4.13}$$

$$T_s(z,t) = \overline{T_s}(z,t) \quad \text{on} \quad \Gamma_h^D \tag{4.14}$$

$$q_w(z,t) = \overline{q_w}(z,t) \quad \text{on} \quad \Gamma_w^N \tag{4.15}$$

$$q_h(z,t) = \overline{q_h}(z,t) \quad \text{on} \quad \Gamma_h^N \tag{4.16}$$

where $\theta_0(z)$ and $T_0(z)$ are the initial value of the volumetric water content and soil temperature, respectively, Ω space domain, $\overline{\theta}(z,t)$ and $\overline{T_s}(z,t)$ the value of the volumetric water content and soil temperature on the Dirichlet boundary, respectively, Γ_w^D and Γ_h^D the Dirichlet boundary for the water and heat movement, respectively, $\overline{q_w}(z,t)$ and $\overline{q_h}(z,t)$ the water and heat flux on the Neumann boundary, respectively and Γ_w^N and Γ_h^N the Neumann boundary for the water and heat movement, respectively. Given that the coefficients of the derivatives in Eqs.(4.1) and (4.7) are well parameterized or related to the unknown variables θ and T_s, such a equations system can be numerically solved with respect to θ and T_s by the combined use of the standard Galerkin finite element method and the implicit time-marching scheme, *i.e.*, Crank-Nicolson scheme. This forward solution model is embedded in the parameter optimization process described below.

4.2.3 Parameterization of soil hydraulic properties

With the observed volumetric water content and suction data collected from data loggers of soil moisture probes and tensiometers which are in the same depth from the ground surface, a scatter diagram relating volumetric water content to suction is obtained. To represent in a functional form the relation between them, or to obtain a soil water retention curve, VG model is employed which is described as follows.

$$S_e = \frac{\theta - \theta_r}{\theta_s - \theta_r} = \frac{1}{(1 + (\alpha_{vg}|\psi|)^{n_{vg}})^{m_{vg}}} \tag{4.17}$$

where S_e is the effective saturation, θ_r the residual water content and α_{vg}, m_{vg} and n_{vg} the unknown parameters, the last two being related as $m_{vg} = 1 - 1/n_{vg}$. To determine values of the parameters in Eq.(4.17) so as to best fit the observed θ-ψ relations, the least-square approach is used (Takeshita and Kohno, 1993[52]).

For functional representation of RHC, a free-form parameterization method is used. For the free-form parameterization, the relation must be expressed by a function which is continuously differentiable over the whole effective saturation domain of interest. For this purpose, as shown in Figure 4.2, the effective saturation domain is partitioned into (I-1) subdomains with I nodes (I denotes the degrees of freedom of the parameterization), and the function for $K_r^{FFP}(S_e)$ over the whole domain $[S_e(\theta_r), S_e(\theta_s)]$ is expressed by a sequence of piecewise cubic spline interpolation functions each of which is locally defined over a confined subdomain bounded with two nodes. Thus the function defined over

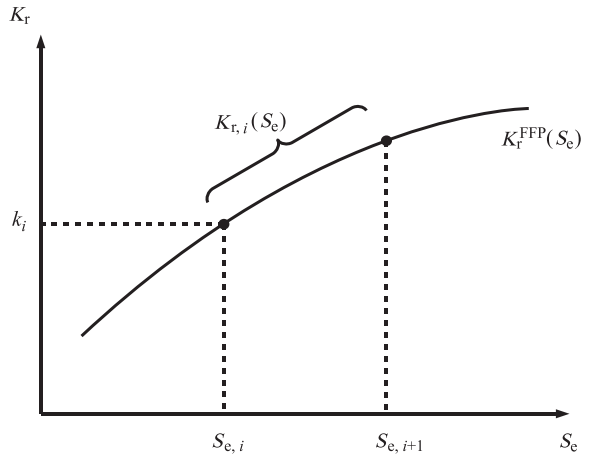

Figure 4.2: Free-form parameterization

the i-th subdomain of $[S_{e,i}, S_{e,i+1}]$, $K_{r,i}(S_e)$, is described as follows.

$$K_r^{FFP}(S_e) = \sum_{i=1}^{I-1} K_{r,i}(S_e) \tag{4.18}$$

with

$$K_{r,i}(S_e) = \begin{cases} a_i + b_i(S_e - S_{e,i}) + c_i(S_e - S_{e,i})^2 \\ \quad + d_i(S_e - S_{e,i})^3, S_e \in [S_{e,i}, S_{e,i+1}] \\ 0, \qquad\qquad S_e \notin [S_{e,i}, S_{e,i+1}] \end{cases} \tag{4.19}$$

where a_i, b_i, c_i and d_i are coefficients in the cubic splines and i $(1 \le i \le I)$ a nodal number. Hereinafter, the values of $K_r^{FFP}(S_e)$ at a node i are simply denoted by k_i and its sets by $\boldsymbol{k}$. Since, as well known, RHC monotonously increases with the increasing saturation, Eq. (4.18) must be identified so that the following constraints are satisfied.

$$k_i \le k_{i+1} \tag{4.20}$$

4.2.4 Inverse problem and solution procedure

The problem is to optimally decide a set of variables, $\boldsymbol{k}$, defined as follows.

$$\boldsymbol{k} = \{k_i, 1 \le i \le I\} \tag{4.21}$$

Searching for the set of the optimal solutions, $\boldsymbol{k}^{opt}$, is then achievable through minimizing the objective function, defined as the total least squares error integrated over space and time between the solution of FP ($\theta^{com}(\boldsymbol{k})$) and the observed data (θ^{obs}), and therefore, written as

$$J(\boldsymbol{k}^{opt}) = \min J(\boldsymbol{k}), \boldsymbol{k}^{opt}, \boldsymbol{k} \in K_{ad} \tag{4.22}$$

with

$$J(\boldsymbol{k}) = \frac{1}{2}\sum_{l=1}^{L} \{f_l(\boldsymbol{k})\}^2 \tag{4.23}$$

$$f_l(\boldsymbol{k}) = w_l(\theta_l^{com}(\boldsymbol{k}) - \theta_l^{obs}) \tag{4.24}$$

where K_{ad} is an admissible set of $\boldsymbol{k}$, L the total number of observed data available in space and time and w_l (normally, taken as unity) a weighting factor.

In the process of minimizing Eq.(4.23) subject to Eq. (4.21), the decision variables $\boldsymbol{k}$ are iteratively updated while step by step solving FP with their assumed or previously estimated values. In this respect, identification of the function (Eq.(4.18)) requires a sort of simulationoptimization technique.

Levenberg-Marquardt method, which is a modified Gauss-Newton method, is adopted for the optimization algorithm. With this method, the unknown parameters are step by step updated with the following search sequence through the iteration.

$$\boldsymbol{k}^{(\gamma+1)} = \boldsymbol{k}^{(\gamma)} + \Delta\boldsymbol{k}^{(\gamma)} \tag{4.25}$$

with

$$\Delta\boldsymbol{k}^{(\gamma)} = -(\boldsymbol{H}^{(\gamma)} + \eta\boldsymbol{I})^{-1}\nabla J^{(\gamma)} \tag{4.26}$$

$$\boldsymbol{H}^{(\gamma)} = \left[\sum_{l=1}^{L} \frac{\partial f_l^{(\gamma)}}{\partial k_i}\frac{\partial f_l^{(\gamma)}}{\partial k_j}\right] \tag{4.27}$$

where γ is an iteration number, η a coefficient and $\boldsymbol{I}$ the $I \times I$ unit matrix. When η is equal to zero, $\Delta\boldsymbol{k}^{(\gamma)}$ reduces to the Gauss-Newton direction. On the other hand, when η tends to infinity, $\Delta\boldsymbol{k}^{(\gamma)}$ turns to the steepest descent direction and size of $\Delta\boldsymbol{k}^{(\gamma)}$ tends to zero. The coefficient η is therefore taken as zero for an initial value, and if $J(\boldsymbol{k}^{(\gamma+1)}) < J(\boldsymbol{k}^{(\gamma)})$ is not satisfied, then value of η is increased and $\Delta\boldsymbol{k}^{(\gamma)}$ is recomputed with Eq.(4.26) until $J(\boldsymbol{k}^{(\gamma+1)}) < J(\boldsymbol{k}^{(\gamma)})$ is satisfied (Sun, 1994[51]).

4.3 Validation

Validity of the inverse method described above is examined through its *in-situ* application to the test soil (sandy soil) in an upland crop field in Miyoshi, Aichi Prefecture. Primarily the examination is made on performance of calibrating the numerical forward solution model—obtained from coupled Eqns.(4.1) and (4.7)—through identifying free-form parameterized RHC function with the *in-situ* observation data, as well as on reproducibility of the forward solutions obtained from the model so calibrated. The validity is then verified in comparison with the method commonly used for identifying RHC. In addition, efficacy of allowing for soil temperature variability—non-isothermal condition—in the forward problem is examined in comparison with making the isothermal assumption valid. The following are preparatory descriptions for these examinations.

As a basis for comparison in parameterization for RHC, the conventional method using VG model of a fixed-form, "VG method", is considered in that RHC expressed in terms of the effective saturation is given as follows.

$$K_r^{VG}(S_e) = S_e^{1/2}\left(1 - (1 - S_e^{1/m_{vg}})^{m_{vg}}\right)^2 \tag{4.28}$$

If the isothermal assumption is accepted or Eq.(4.1) is

uncoupled from Eq.(4.7), the governing equation for FP is simplified with independence of soil temperature as follows.

$$\rho_w \frac{\partial \theta}{\partial t} = -\frac{\partial q_w}{\partial z} \tag{4.29}$$

$$q_w = -\rho_w D_\theta \frac{\partial \theta}{\partial z} - \rho_w K \tag{4.30}$$

$$D_\theta = K \frac{\partial \psi}{\partial \theta} = \frac{K}{C_w} \tag{4.31}$$

$$K = K_r K_s \tag{4.32}$$

where K_s takes a constant value at soil temperature of 15 ℃. RHC, K_r, is estimated in the same manner as in the non-isothermal case.

4.3.1 Field observation and soil water retention curve fitting

The observation system with full instruments, as shown in Figure 4.3, was *in-situ* set up. The target domain is the surface soil of 20 cm thick—from -10 cm to -30 cm—, where soil temperature varies perceptibly. Assumed predominantly one-dimensional, the domain of a soil column is divided into four equal elements with five nodes. The instruments sense and automatically record at intervals of 10 min the variations of volumetric water content, suction and soil temperature at each depth of 10 cm, 20 cm and 30 cm below the ground level. To know the response of soil moisture variation to occurrence of rainfall events, an automatic rain gauge is placed close by the system to record time-varying precipitation at the same time interval.

The complete serial data of volumetric water content, suction and soil temperature, observed during the period of June 8, 2008 to July 9, 2008 and selected for the present examinations, are illustrated in Figure 4.4 including that of the rainfall. Here, a one-way process of desorption is considered for the estimation of the soil hydraulic properties. The distinct desorption periods, detectable at a glance from the suction variation in Figure 4.4, are those of June 12 to 19, June 24 to 28 and July 1 to 8. These are considered as mutually independent time sequences to provide the different sets of the observed serial data and thus to make more persuasive examinations of the present propositions.

The examinations must be preceded by finding the soil water retention curve Eq.(4.17), for each desorption period, best fitting the scattered relations between observed θ and ψ. Here, θ_s is taken as the value for $\psi = 0$, and θ_r as the minimum value found in all the observed serial data of θ, including the data shown in Figure 4.4. Thus, values of θ_s and θ_r can directly be identified to be 0.48 and 0.22, as common to three different desorption periods, through analyzing the observed serial data of ψ and θ, and of θ, respectively. Caution must be paid in identifying values of α_{vg} and n_{vg} by use of the least squares method. Theory predicts that ψ and θ are uniquely correlated, or that, if under the same

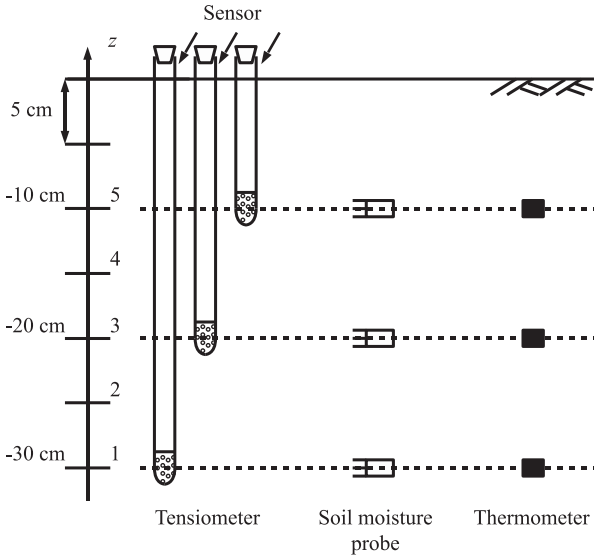

Figure 4.3: Full instrumentation

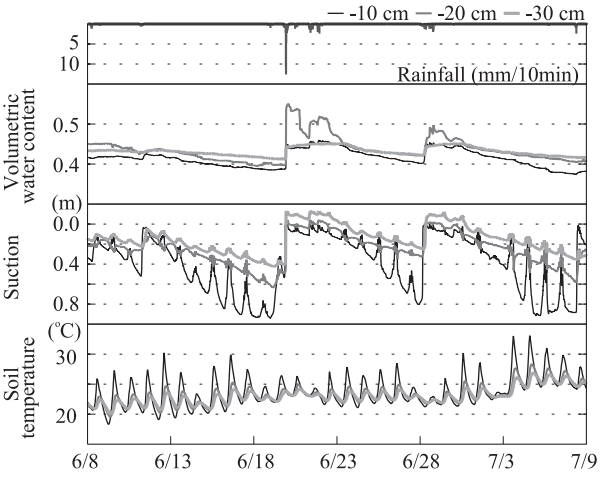

Figure 4.4: Observed data

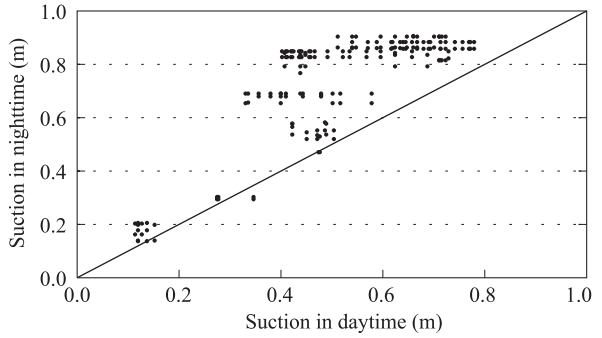

Figure 4.5: Correlation between suctions in daytime and nighttime

situation of the water content, the readings of ψ must be the same. In real observation, however, the daytime and nighttime readings of ψ for the same value of θ are at variance, as exemplified in Figure 4.5, the former being relatively reduced. This is a result of that the suction sensors (UIZ-SMT, UIZIN Co., Ltd.) are positioned near the mouth of a tensiometer tube and therefore prone to

observe the suctions affected by air temperature. For this, the observed θ-ψ relations over the nighttime of 20:00 to 8:00, less affected by air temperature, are exclusively qualified as those to be fitted with a curve, discarding those over the daytime. All the relations qualified and the resulting curves fitted with Eq.(4.17) are illustrated in Figures 4.6 to 4.8 for the respective desorption periods. The resultant identified values of α_{vg} and n_{vg} are listed in Table 4.1 including the value of K_s^{15} that was measured through laboratory tests for the soils sampled from the site.

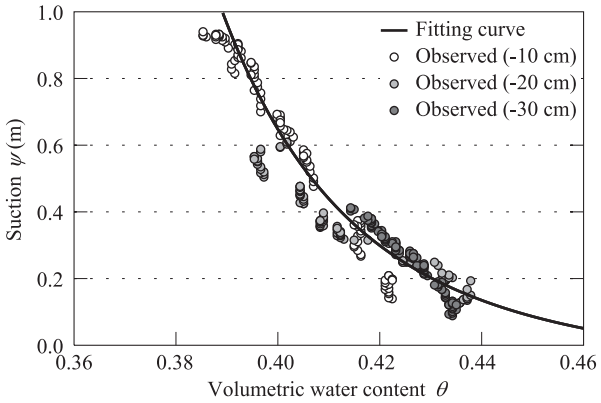

Figure 4.6: Soil water retention property in the first desorption period

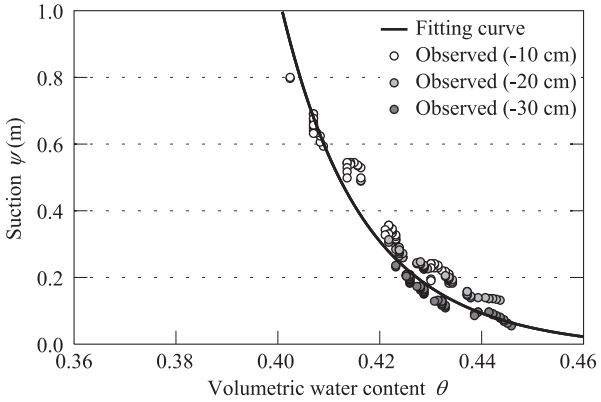

Figure 4.7: Soil water retention property in the second desorption period

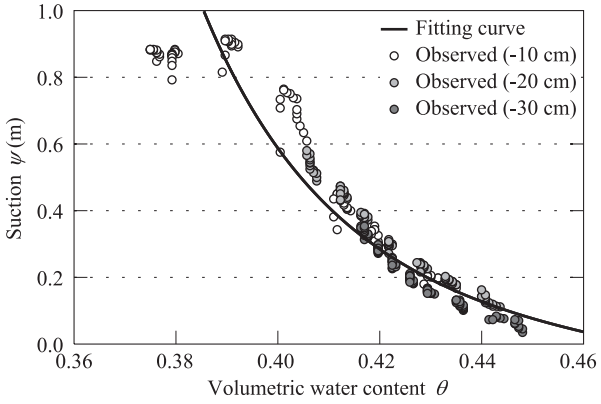

Figure 4.8: Soil water retention property in the third desorption period

Table 4.1: Identified parameter values

Desorption period	K_s^{15} [m/s]	α_{vg} [/m]	n_{vg}
6/12-6/19		17.1	1.142
6/24-6/28	4.5×10^{-4}	49.8	1.084
7/1-7/8		10.3	1.172

K_s^{15} indicates K_s at 15 ℃.

4.3.2 Results and discussion

The results of the examinations concerning calibration of the numerical model and solution reproducibility (accuracy) of the model calibrated are shown in the insert of Figure X (X=4.9, 4.10, 4.11) for the respective desorption periods. Note that for each all the results except for θ^{iso} in Figure X(c) are those for non-isothermal condition. It should be also noted that for all w_l in Eq. (4.24) is equalized to unity. Figure X(a) comparatively illustrates the RHC functions K_r^{FFP} and K_r^{VG} which were identified by the present free-form parameterization and the fixedform parameterization based on the VG model, respectively. Including the time-varying θ^{obs} observed at the intermediate depth of the soil column, Figure X(b) shows the corresponding θ^{com} and θ^{VG} computed as the solutions of FP with the identified K_r^{FFP} and K_r^{VG}, respectively. In the lower half of the same, the absolute errors $E^{com}=|\theta^{com}-\theta^{obs}|$ and $E^{vg}=|\theta^{vg}-\theta^{obs}|$ are shown to demonstrate the time-varying difference in solution reproducibility between free- and fixed-form parameterizations. Figure X(c) illustrated in the same manner as in Figure X(b) is inserted to differentiate the non-isothermal solution θ^{com} from the isothermal solution θ^{iso} produced with the identified K_r^{FFP}. The daily periodic variations of computed T_s^{com} and observed T_s^{obs} at the intermediate depth are comparatively shown in Figure X (d), including the time-varying soil temperatures observed at the top ($z=-0.1$) and bottom ($z=-0.3$) of the soil column, which are given as Dirichlet boundary values in solving FP. Minimum values of the objective function $J(\boldsymbol{k})$, which are reached in simulation-optimization processes for identifying RHC function K_r and thus could be a global indicator of solution reproducibility, are summarized in Table 4.2, including those for the three different combinations of free- or fixed-form parameterization and isothermal or non-isothermal setting for each of the different three desorption periods.

From Figures 4.9(a), 4.10(a) and 4.11(a), it can readily be seen that the shape of the function $K_r(S_e)$ is relaxed in the free-form parameterization, turning upward at a lower level of effective saturation than in the conventional fixed-form parameterization. From Figures 4.9(b), 4.10(b) and 4.11(b), it can be recognized that the model calibrated with such a parameter identification technique reproduces the forward solutions in better agreement with the observed data. Table 4.2 demonstrates in a quantitative sense that this is indeed true for any of desorption periods. This could be strong evidence that the method presently developed for solving IP surpasses the

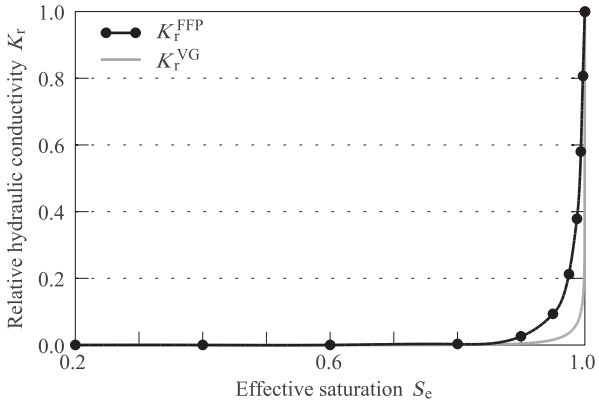

(a)

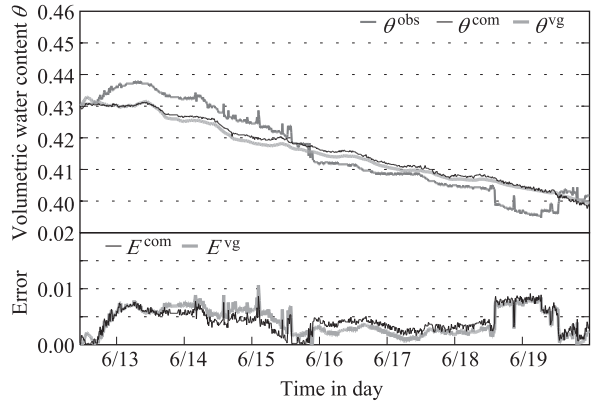

(b)

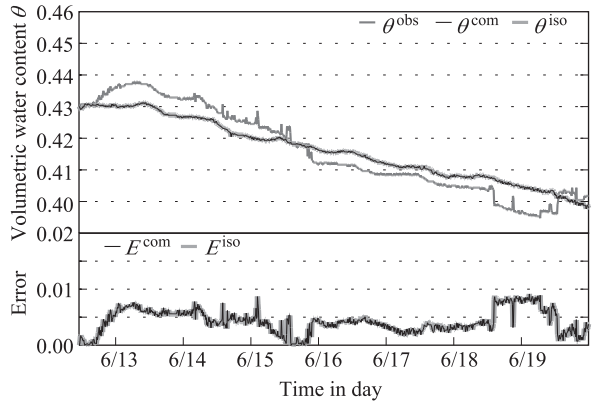

(a)

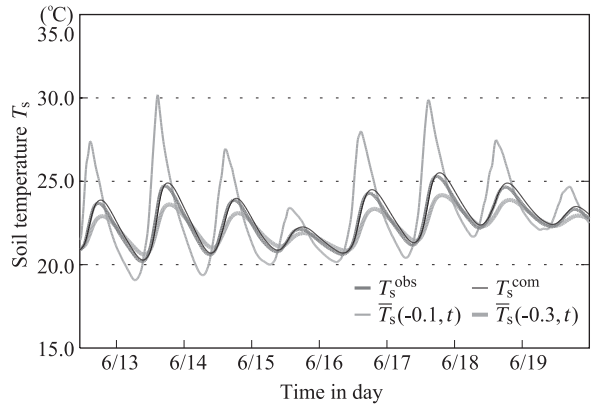

(a)

Figure 4.9: Calibration result for the first desorption period

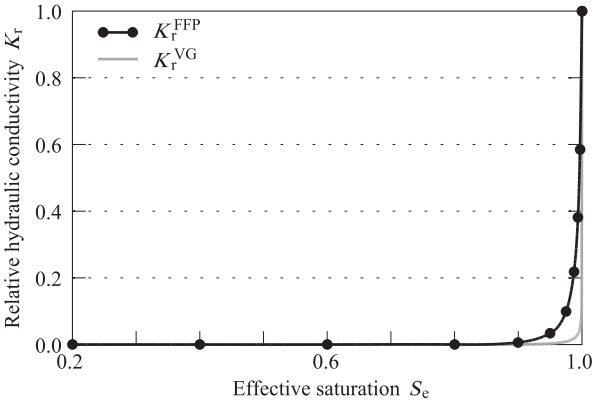

(a)

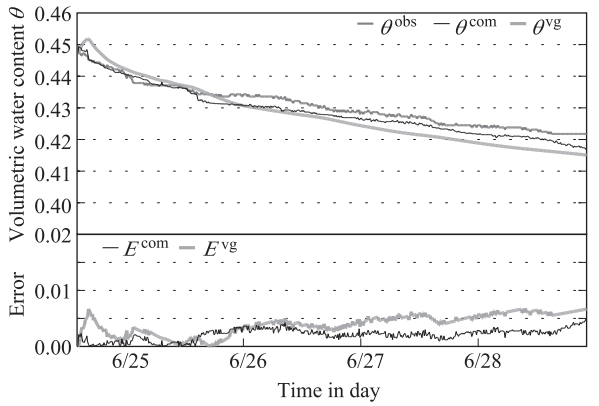

(b)

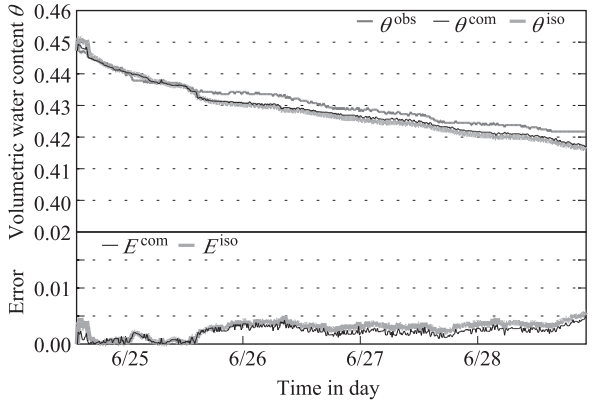

(c)

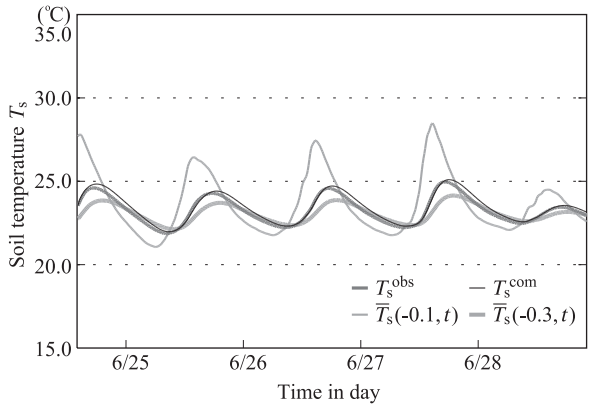

(d)

Figure 4.10: Calibration result for the second desorption period

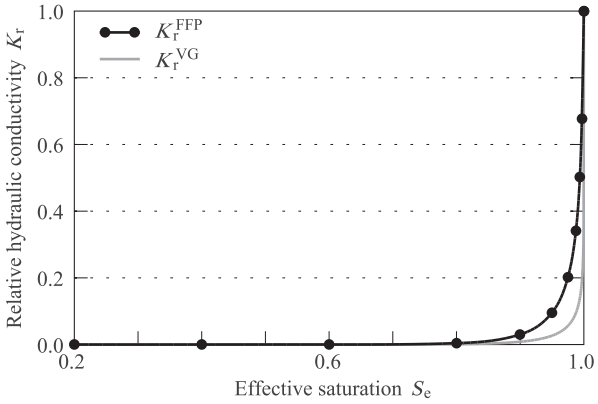

(a)

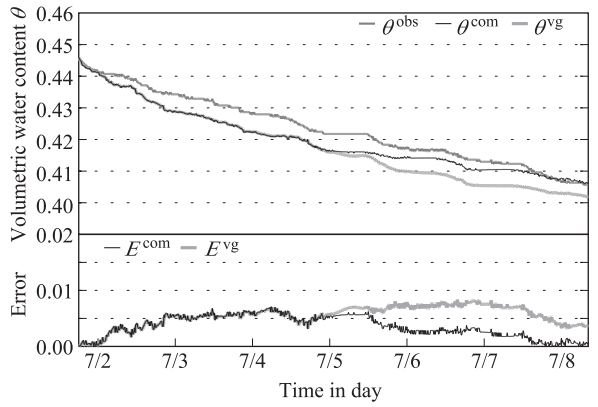

(b)

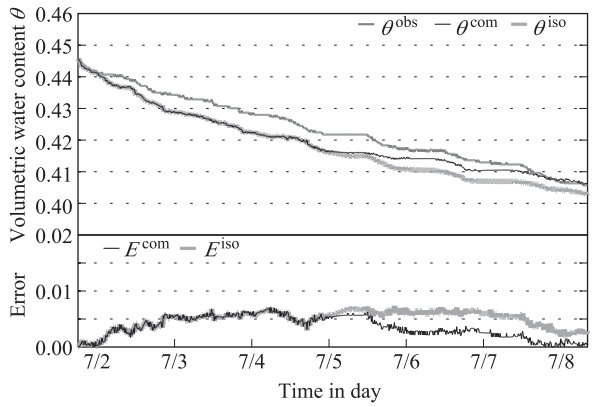

(c)

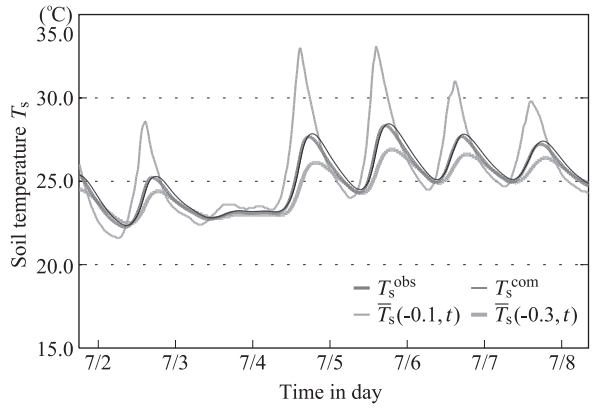

(d)

4.11: Calibration result for the third desorption period

commonly used one which employs the well-defined VG model for identification of RHC. From Figures 4.9(c), 4.10(c), 4.11(c) and Table 4.2, it is also found that taking into account the non-isothermal condition leads to the increase in solution closeness to reality.

Table 4.2: Minimum values of $J(\boldsymbol{k})$ in simulation-optimizarion runs for different periods

Desorption period	6/12-6/19	6/24-6/28	7/1-7/8
Non-isothermal/free-form	0.0239	0.00345	0.0144
Non-isothermal/fixed-form (VG)	0.0247	0.0118	0.0315
Isothermal/free-form	0.0242	0.00597	0.0258

4.4 Conclusions

A method for solving the inverse problem of variably saturated seepage flow in non-isothermal soil has been developed. A utilitarian *in-situ* observation system with simple instrumentation has specially been contrived which implements collection of the data necessary for solving the inverse problem. The results of the examinations on validity of the method reveals that the relative hydraulic conductivity of major parameter, described as a function of the effective saturation, could successfully be identified with a free-form continuous function formed by a sequence of piecewise cubic spline functions whose coefficients are found with the aid of the simulation-optimization technique. The results also show that the water movement model provides the forward solutions of high reproducibility, when coupled with thermal conduction model and calibrated through identifying the relative hydraulic conductivity with such a freeform function in lieu of a fixed-form function. It is thus concluded that the present approach of taking into account the effect of thermal conduction on water movement in variably saturated soil and employing the free-form parameterization technique could be the viable alternative to the conventional tedious and laborious approaches. Additionally it should be mentioned that the inexpensive observation system specially contrived enhances usefulness of the approach.

CHAPTER 5

INVERSE METHOD TO IDENTIFY UNSATURATED HYDRAULIC CONDUCTIVITY IN VARIABLY SATURATED SUBSURFACE WATER FLOW MODEL —MIXED FORM OF RICHARDS EQUATION—

5.1 Introduction

Richards equation can be expressed in three different forms according to the state variables solved: the ψ-based form, the θ-based form, and the mixed form. Since the θ-based form is not applicable for the saturated zones where the hydraulic diffusivity takes infinite values, the ψ-based form which can express all possible ranges of saturation is often used. However, Celia *et al*. (1990)[6] reported that numerical models which solve ψ-based form produce significant errors in mass balance, and proposed an alternative model which solves the mixed form perfectly conserving the mass. After the work of Celia *et al*. (1990)[6], the mixed form of Richards equation is often used as the governing equation for seepage flow, and the computational efficiency of its numerical model is improved (Huang *et al*., 1996)[19]. Almost all the numerical models proposed by Celia *et al*. (1990)[6], and subsequently others, deal with only unsaturated zone, while Takeuchi *et al*. (2008)[54] developed a numerical model which can solve the mixed form of Richards equation for saturated zone as well as for unsaturated zone.

Izumi *et al*. (2008[28], 2009[27]) have developed inverse modeling for both the ψ-based form and θ-based form of Richards equation. In this chapter, an inverse modeling for the mixed form using the free-form parameterization technique is proposed. Firstly, the FP employing the mixed form of Richards equation as the governing equation is defined. Because the saturated hydraulic conductivity could be definitely known, the IP related to the unsaturated hydraulic conductivity is reduced to a problem of identifying the RHC. Secondly, RHC is represented by a free-form parameterized function which is a sequence of piecewise cubic spline functions over the whole effective saturation domain. Thirdly, the inverse problem of minimizing errors between the observed and computed values of the pressure head is formulated based on a simulation-optimization algorithm with the aid of the Levenberg-Marqurdt method to find optimal values of the parameters included in the RHC function. Finally, the inverse method developed is validated through applying it for *in-situ* soil column in an upland crop field and comparing the observed water movement with the computed one obtained from the forward simulation for the desorption process in that considering the hysteric phenomenon is not needed.

5.2 Forward Problem

5.2.1 Governing equation

The subsurface water flow in variably saturated soil can be described by Richards equation which combines the mass conservation equation and the Darcy-Buckingham's law, and its mixed form is represented as follows (Huyakorn and Pinder, 1983[20]).

$$\phi \frac{\partial S_w}{\partial t} + S_w S_s \frac{\partial \psi}{\partial t} = -\frac{\partial}{\partial z}\left(-K\frac{\partial h}{\partial z}\right) \tag{5.1}$$

with

$$S_s = \rho_w g\,(\beta_s + \phi\beta_w) \tag{5.2}$$

$$K = K_r K_s \tag{5.3}$$

where ϕ is the porosity, S_w the saturation, S_s the specific storage, ψ the pressure head, K the unsaturated hydraulic conductivity, $h\ (=\psi+z)$ the hydraulic head, t the time, z the height defined as positive upward, ρ_w the water density assumed to be constant here, g the gravitational acceleration, β_s and β_w the compressibility coefficients of soil and water, respectively, K_r the relative hydraulic conductivity and K_s the saturated hydraulic conductivity.

Eq.(5.1) is subject to the following initial and boundary conditions.

$$\psi(z,0) = \psi_0(z) \qquad \text{in} \quad \Omega \tag{5.4}$$

$$\psi(z,t) = \overline{\psi}(z,t) \qquad \text{on} \quad \Gamma^D \tag{5.5}$$

$$-K_s K_r \frac{\partial h}{\partial z} = \overline{q}(z,t) \qquad \text{on} \quad \Gamma^N \tag{5.6}$$

where $\psi_0(z)$ is the initial value of the pressure head in the space domain Ω, $\overline{\psi}(z,t)$ the value of the pressure head on the Dirichlet boundary Γ^D and $\overline{q}(z,t)$ the water flux on the Neumann boundary Γ^N.

Given that the coefficients of the derivatives in Eq.(5.1) is well parameterized or related to the unknown variables ψ, such a equations system can be numerically solved with respect to ψ by the combined use of the standard Galerkin finite element method and the fully implicit time-marching scheme mentioned below. This forward solution procedure is embedded in the parameter optimization process.

5.2.2 Parameterization of soil hydraulic properties

To represent a constitutive relation between the volumetric water content and pressure head, or to obtain a soil water retention curve, VG model is employed which is described as follows.

$$S_e = \frac{\theta-\theta_r}{\theta_s-\theta_r} = \frac{1}{(1+(\alpha_{vg}|\psi|)^{n_{vg}})^{m_{vg}}} \tag{5.7}$$

where S_e is the effective saturation, θ the volumetric water content, θ_r the residual water content, θ_s the saturated water content and α_{vg}, m_{vg} and n_{vg} the unknown parameters, the last two being related as $m_{vg} = 1 - 1/n_{vg}$. To determine values of the parameters in Eq.(5.7) so as to best fit the observed θ-ψ relations, the least-square

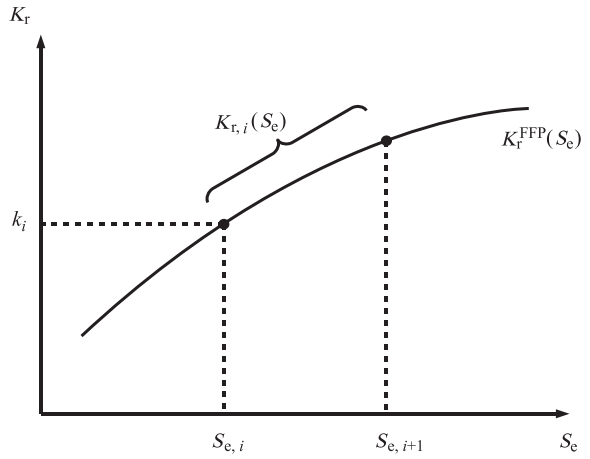

Figure 5.1: Free-form parameterization

approach is used.

For functional representation of RHC, the free-form parameterization method is employed. For such a parameterization, the relation must be expressed by a function which is continuously differentiable over the whole effective saturation domain of interest. For this, as shown in Figure 5.1, the effective saturation domain is partitioned into $(I-1)$ sub-domains with I nodes (I denotes the degrees of freedom of the parameterization), and the function for $K_r^{FFP}(S_e)$ over the whole domain $[S_e(\theta_r)=0,\ S_e(\theta_s)=1]$ is expressed by a sequence of piecewise cubic spline functions each of which is locally defined over a confined sub-domain bounded with two nodes. Thus, the function defined over the i th sub-domain of $[S_{e,i}, S_{e,i+1}]$, $K_{r,i}(S_e)$ is described as follows.

$$K_r^{FFP}(S_e)=\sum_{i=1}^{I-1} K_{r,i}(S_e) \tag{5.8}$$

with

$$K_{r,i}(S_e)=\begin{cases} a_i^k+b_i^k(S_e-S_{e,i})+c_i^k(S_e-S_{e,i})^2 \\ \quad +d_i^k(S_e-S_{e,i})^3, S_e\in[S_{e,i}, S_{e,i+1}] \\ 0, \qquad\qquad S_e\notin[S_{e,i}, S_{e,i+1}] \end{cases} \tag{5.9}$$

where a_i^k, b_i^k, c_i^k and d_i^k are coefficients in the cubic splines and $i\ (1\le i\le I)$ a nodal number. Hereinafter, the values of $K_r^{FFP}(S_e)$ at a node i are simply denoted by k_i. Since, as well known, the relative hydraulic conductivity monotonously increases with the increasing saturation, Eq. (5.8) must be identified so that the following constraints are satisfied.

$$k_i \le k_{i+1} \tag{5.10}$$

5.2.3 Time-marching scheme

The governing equation is discretized by a standard Galerkin finite element method for space and a finite difference method for time. As the time-marching scheme, the modified Picard method proposed by Celia *et al*. (1990)[6] is used. If the superscripts m and n stand for an iteration step and a time level, respectively, then the Picard iteration scheme can be written as

$$\frac{S_w^{n+1,m+1}-S_w^n}{\Delta t}+\frac{S_w^{n+1,m}S_s}{\phi}\frac{\psi^{n+1,m}-\psi^n}{\Delta t} -\frac{1}{\phi}\left(\frac{\partial}{\partial z}\left(K^{n+1,m}\frac{\partial\psi^{n+1,m}}{\partial z}\right)-\frac{\partial K^{n+1,m}}{\partial z}\right)=0 \tag{5.11}$$

According to Celia *et al*. (1990)[6], $S_w^{n+1,m+1}$ is expanded with respect to ψ by Taylor series expansion, ignoring the higher order, as follows.

$$\begin{aligned} S_w^{n+1,m+1} &= S_w^{n+1,m}+\left.\frac{dS_w}{d\psi}\right|^{n+1,m}(\psi^{n+1,m+1}-\psi^{n+1,m}) \\ &= S_w^{n+1,m}+\frac{C_w^{n+1,m}}{\phi}(\psi^{n+1,m+1}-\psi^{n+1,m}) \end{aligned} \tag{5.12}$$

where C_w is the specific water content. Substituting the truncated series Eq.(5.12) into Eq.(5.11)

$$\psi^{n+1,m+1}=\psi^{n+1,m}+\Delta t\frac{\phi}{C_w^{n+1,m}}\left(-\frac{S_w^{n+1,m}-S_w^n}{\Delta t} -\frac{S_w^{n+1,m}S_s}{\phi}\frac{\psi^{n+1,m}-\psi^n}{\Delta t}+\frac{1}{\phi}\left(\frac{\partial}{\partial z}\left(K^{n+1,m}\frac{\partial\psi^{n+1,m}}{\partial z}\right) +\frac{\partial K^{n+1,m}}{\partial z}\right)\right) \tag{5.13}$$

When a soil domain of interest is saturated, S_w = const. $=1$. Thus, the first term on the left-hand side of Eq.(5.1) disappears, and the equation becomes as follows.

$$S_s\frac{\partial\psi}{\partial t}=-\frac{\partial}{\partial z}\left(-K\frac{\partial h}{\partial z}\right) \tag{5.14}$$

Employing the modified Picard scheme, Eq.(5.14) can be written in the time-marching form as follows.

$$\psi^{n+1,m+1}=\psi^n+\Delta t\frac{1}{S_s}\left(\frac{\partial}{\partial z}\left(K^{n+1,m}\frac{\partial\psi^{n+1,m}}{\partial z}\right) +\frac{\partial K^{n+1,m}}{\partial z}\right) \tag{5.15}$$

5.3 Inverse Problem

5.3.1 Formulation of optimization problem

Solving IP is defined as optimally deciding a set of unknown variables, $\boldsymbol{k}=\{k_i, 1\le i\le I\}$. The objective function is then defined as the total least squares error integrated over space and time between the solution of FP ($\psi^{com}(\boldsymbol{k})$) and the observed data (ψ^{obs}), and therefore, written as

$$J(\boldsymbol{k}^{opt})=\min J(\boldsymbol{k}),\quad \boldsymbol{k}\in K_{ad} \tag{5.16}$$

with

$$J(\boldsymbol{k})=\frac{1}{2}\sum_{l=1}^{L}\{f_l(\boldsymbol{k})\}^2 \tag{5.17}$$

$$f_l(\boldsymbol{k})=w_l(\psi_l^{com}(\boldsymbol{k})-\psi_l^{obs}) \tag{5.18}$$

where $\boldsymbol{k}^{opt}$ is a set of $\boldsymbol{k}$ optimal solutions, K_{ad} an admissible set of $\boldsymbol{k}$, L the total number of observed data available in space and time and w_l (normally, taken as unity) a weighting factor.

In the process of minimizing Eq.(5.17) subject to Eq. (5.10), the decision variables, $\boldsymbol{k}$, are iteratively updated while step by step solving FP with their assumed or previously estimated values. In this respect, identification of the function (Eq.(5.8)) requires a sort of simulation-optimization technique.

5.3.2 Optimization algorithm

For the optimization algorithm to search for the set of the optimal solutions, $\boldsymbol{k}^{\mathrm{opt}}$, Levenberg-Marquardt method, which is a modified Gauss-Newton method, is adopted. With this method, the unknown parameters are step by step updated with the following search sequence through the iteration.

$$\boldsymbol{k}^{(\gamma+1)} = \boldsymbol{k}^{(\gamma)} + \Delta\boldsymbol{k}^{(\gamma)} \tag{5.19}$$

with

$$\Delta\boldsymbol{k}^{\gamma} = -(\boldsymbol{H}^{\gamma} + \eta\boldsymbol{I})^{-1}\nabla J^{(\gamma)} \tag{5.20}$$

$$\boldsymbol{H}^{(\gamma)} = \left[\sum_{l=1}^{L}\frac{\partial f_l^{(\gamma)}}{\partial k_i}\frac{\partial f_l^{(\gamma)}}{\partial k_j}\right] \tag{5.21}$$

where γ is an iteration number, η a coefficient and $\boldsymbol{I}$ the $I \times I$ unit matrix. When η is equal to zero, $\Delta\boldsymbol{k}^{(\gamma)}$ reduces to the Gauss-Newton direction. On the other hand, when tends to infinity, $\Delta\boldsymbol{k}^{(\gamma)}$ turns to the steepest descent direction and size of $\Delta\boldsymbol{k}^{(\gamma)}$ tends to zero. Therefore, η is taken as zero for an initial value, and if $J(\boldsymbol{k}^{(\gamma+1)}) < J(\boldsymbol{k}^{(\gamma)})$ is not satisfied, then value of η is increased and $\Delta\boldsymbol{k}^{(\gamma)}$ is recomputed with Eq.(5.20) until $J(\boldsymbol{k}^{(\gamma+1)}) < J(\boldsymbol{k}^{(\gamma)})$ is satisfied (Sun, 1994[51]).

5.4 Validation

An *in-situ* application to the test soil (sandy soil) in an upland crop field in Miyoshi, Aichi Prefecture, Japan, is implemented to examine validity of the inverse method described above. The validity is judged referring to reproducibility of the forward solutions obtained from the calibrated model.

5.4.1 Observation system

The data necessary for identification of RHC is acquired by the observation system made up of different three sets of instruments (tensiometer and soil moisture probe), which are buried at different three depths in a soil column (Figure 5.2). At individual depths, serial data of pressure head and volumetric water content are observed which are necessary to identify the soil water retention property. The observed pressure heads at both top and bottom of the soil column are also used as Dirichlet boundary values in solving FP based on the governing equation. The pressure head observed at the intermediate depth (-20 cm deep) is used to judge the fitness of estimated unknown parameters (or RHC function) in an optimization process.

The targeted domain is the surface soil of 20 cm thick between -10 cm and -30 cm deep, where soil alternates

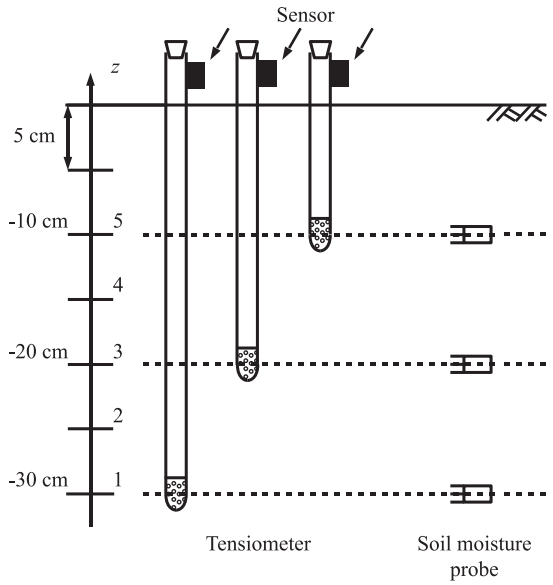

Figure 5.2: Observation system and discretization of targeted domain

between saturated and unsaturated situations with frequency, and is discretized into four equal elements with five nodes for numerical computations. The time-varying pressure heads and volumetric water contents at the three depths of -10 cm, -20 cm and -30 cm are automatically logged at intervals of 10 minutes.

A one-way process of desorption is considered for estimation of the soil hydraulic properties to exclude the hysteric phenomenon, as in most of the preceding studies associated with parameter identification. The data observed during the no-rainfall period (or desorption period) of July 1 to 9, 2008, used as basic data for calibration of the numerical model as well as for validation of the inverse method presently developed, are illustrated in Figure 5.3. From Figure 5.3, it can readily be seen that the pressure head involves periodic daily variations while declining in time, having a distinct difference from the volumetric water content. Even if the volumetric water contents in daytime and nighttime are

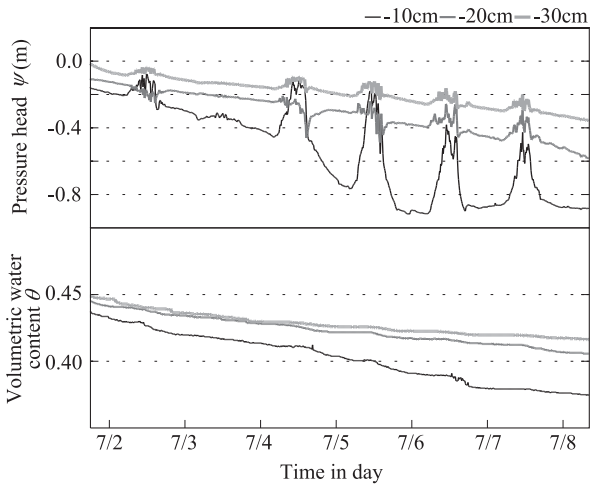

Figure 5.3: Observed data for validation

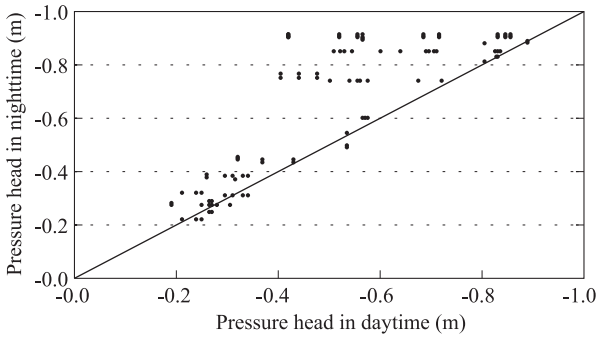

Figure 5.4: Correlation between pressure heads in daytime and nighttime for the same volumetric water content

the same, therefore, the pressure heads are different as shown in Figure 5.4. This result is against the theory that there should be a one-to-one correspondence between the pressure head and the volumetric water content. As Inoue *et al*. (2004)[23] reported, this is because the sensing part of this type of a tensiometer (UIZ-SMT, UIZIN Co., Ltd.) is put near the top of the tube, and therefore the readings of the pressure head are significantly affected by air temperature. Thus, as described later, identification of RHC function is comparatively done considering another data series of the pressure head in which temperature-dependency of the pressure heads in the daytime of 6:00 to 18:00 is removed by means of the linear interpolation method.

5.4.2 Identification of water retention property

Identifying RHC function must be preceded by fixing the form of the soil water retention curve expressed by Eq.(5.7). The saturated water content θ_s is defined as the value of θ in case that ψ is equal to zero, and the residual water content θ_r is defined as the minimum value in all the observed serial data of θ. Thus, straightforwardly from the data observed, θ_s and θ_r can be identified to be 0.45 and 0.22, respectively. By use of the least squares method proposed by Takeshita and Kohno (1993)[52], the remaining parameters α and n_{vg} are determined so that

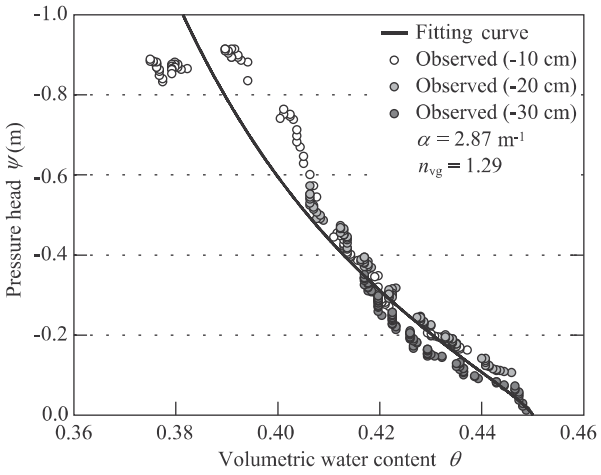

Figure 5.5: Soil water retention property

Eq.(5.7) can be best fit to the observed relations between ψ and θ. Note that in this curvefitting the temperature-dependent θ-ψ relations observed during the daytime of 6:00 to 18:00 are not considered. Eventually the values of α_{vg} and n_{vg} are identified to be 2.87 m^{-1} and 1.29, respectively, to have a best fitting curve as shown in Figure 5.5.

5.4.3 Identification of RHC and validation of the method

As mentioned above, the time-varying pressure head obtained from a field observation is significantly affected by air temperature. Different two data sets of time-varying pressure head are thus considered for identifying RHC (or calibrating the model) by free-form parameterization and examining solution reproducibility (accuracy) of the model so calibrated. One is the observed data as they are, and the other is the corrected data which can be obtained from filtering out daytime temperature-dependent noises from the observed data, or from assuming that the pressure head varies linearly from the observed head at 6:00 to that at 18:00. These are referred to as 〈Data A〉 and 〈Data B〉, respectively.

The value of K_s is given as 4.5×10^{-4} m/s from the result of the laboratory tests for the soils sampled from the site. In application of Eq.(5.18), all w_l are equalized to unity.

The results for 〈Data A〉 and 〈Data B〉 are shown in Figures 5.6 and 5.7, respectively, illustrating the identified RHC function K_r^{FFP} and the solution reproducibility. The solution reproducibility is examined through comparing the computed ψ^{com} (or the forward solution with the identified K_r^{FFP}) with the non-corrected (observed) or corrected ψ^{obs}, and measured in terms of the absolute error $E^{com} = |\psi^{com} - \psi^{obs}|$. Values of the objective function $J(\boldsymbol{k})$, which are reached in the simulation-optimization processes for identifying RHC function and thus could be a global indicator of solution reproducibility, are listed in Table 5.1.

From Figure 5.6 (b), it can be seen that the model calibrated for 〈Data A〉 produces the forward solutions in partially good agreement with the original observed data. From Figure 5.7 (b), on the other hand, it is recognized that the model calibrated for 〈Data B〉 reproduces the corrected observed data in closer agreement. Table 5.1 also demonstrates the same in a quantitative sense. It is thus concluded that the method presently developed could be a viable tool for finding RHC in a functional form, fulfilling its function with better performance if air-temperature dependency of the pressure head variation is appropriately eliminated.

Table 5.1: Minimum values of $J(\boldsymbol{k})$ in simulation-optimization

Data type	$J(\boldsymbol{k})$
〈Data A〉	1.88
〈Data B〉	0.737

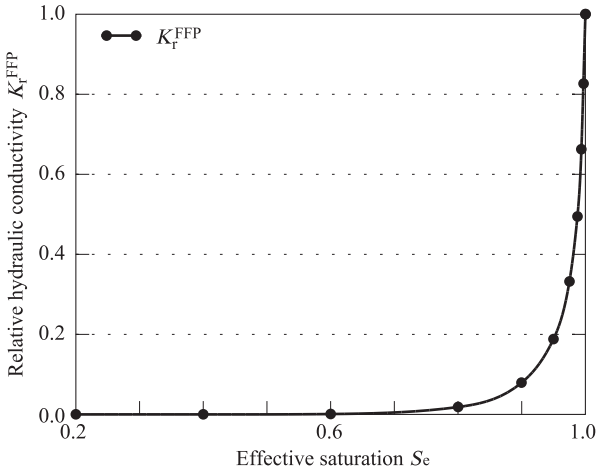

(a)

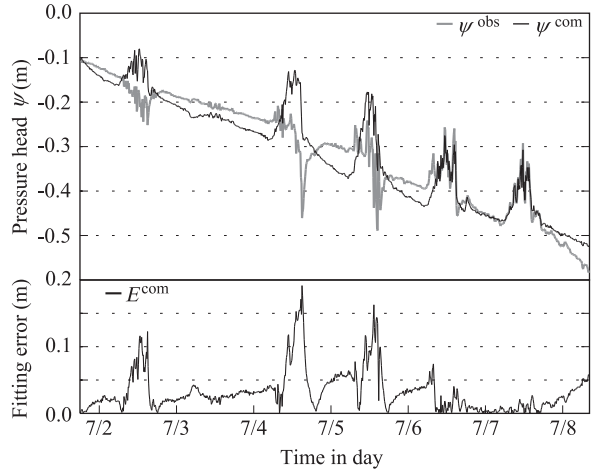

(b)

Figure 5.6: (a) Identified RHC and (b) Reproducibility of FP solution for〈Data A〉

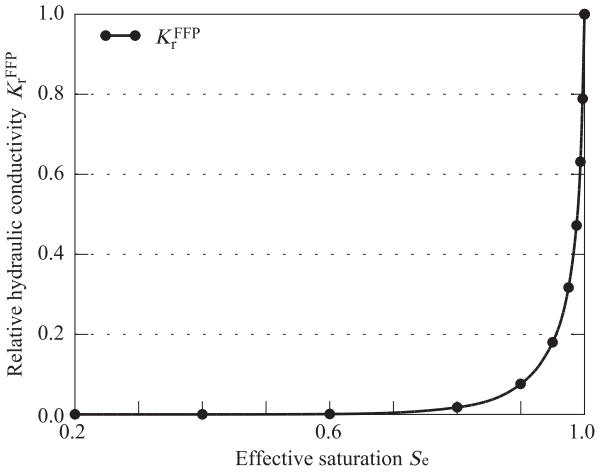

(a)

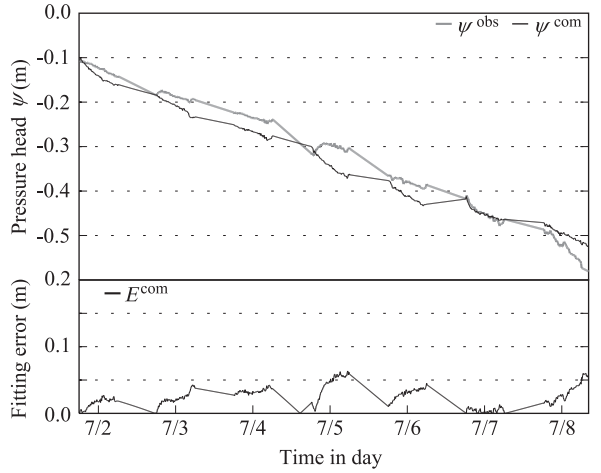

(b)

Figure 5.7: (a) Identified RHC and (b) Reproducibility of FP solution for〈Data B〉

5.5 Conclusions

A method for solving the inverse problem associated with variably saturated seepage flow has been developed. The mixed form Richards equation which provides mass-conservative solutions to saturated-unsaturated seepage flow problem is considered as the governing equation which describes the forward problem. Examinations for validation of the method developed show that the relative hydraulic conductivity which is a major hydraulic property of the governing equation system, expressed by a free-form sequential piecewise cubic spline function, could successfully be identified through determining the values of the coefficients of the function with the aid of the simulation-optimization technique. The results also show that the forward solution model with identified relative hydraulic conductivity could reproduce actual one-way desorption process with higher accuracy when air-temperature dependency of the observed pressure head variation is appropriately eliminated.

CHAPTER 6

INVERSE METHOD TO IDENTIFY UNSATURATED HYDRAULIC CONDUCTIVITY IN VARIABLY SATURATED SUBSURFACE WATER FLOW MODEL IN NON-ISOTHERMAL SOIL —MIXED FORM OF RICHARDS EQUATION—

6.1 Introduction

Richards equation expresses the water movement through soil derived from the gradient of hydraulic head under isothermal assumption. However, water movement is also affected by soil temperature. Thus, this equation is not suitable to represent water movement, especially, near surface soil where heat energy exchange is quite significant. As extended models, coupling models for simultaneous transfer of water and heat based on the work of Philip and de Vries (1957)[46] have been proposed (*e.g.,* Milly, 1982[36]; Kondo and Saigusa, 1994[33]). Fujinawa (1995, 2010)[14],[15] proposed another coupling model. While these models are related to the ψ-based form or θ-based form of Richards equation coupled with heat transport equation, few coupling models of the mixed form of Richards equation and the heat transport equation has been studied. In this chapter, thus, an inverse modeling for the mixed form of Richards equation in non-isothermal soil is purposed. Firstly, the governing equations system (*i.e.,* FP) is described, and the soil hydraulic properties which are model parameters included in the system are parameterized. The RHC which is a major unknown parameter to be identified in this study is described by a free-form parameterized function which is a sequence of piecewise cubic spline functions over the whole effective saturation domain. For the representation of SWRC, VG model is employed due to being time-proven. Secondly, the IP is defined as minimizing errors between the observed and computed values of the pressure head based on a simulation-optimization algorithm with the aid of the Levenberg-Marqurdt method to determine the functional shape of RHC. Finally, the applicability of the inverse method developed is assessed through *in-situ* soil column experiments in terms of reproducibility for observed water movement during the desorption process in that considering the hysteric phenomenon is not needed.

6.2 Governing Equations System

6.2.1 Water movement model

For the water movement, the mixed form of Richards equation derived from the generalized Darcy's law and the Boussinesq assumption (Huyakorn and Pinder, 1983[20]) is employed to obtain the mass-conservative numerical solutions. Considering the dependency of density and viscosity of water on soil temperature to couple with thermal transport, the equation in onedimensional vertical and saturated-unsaturated flow which in the liquid phase has considerable magnitude, *i.e.,* neglecting the vapor fluxes, is described as follows;

$$\phi \frac{\partial S_w}{\partial t} + S_w S_s \frac{\partial \psi}{\partial t} = -\frac{\partial}{\partial z}\left(-K\left(\frac{\partial h}{\partial z} + \frac{\rho_T - \rho_r}{\rho_r}\right)\right) \quad (6.1)$$

with

$$S_s = \rho_r g\,(\beta_s + \phi\beta_w) \quad (6.2)$$

$$K = K_r(S_e)\,K_T(T_s)\,K_s \quad (6.3)$$

$$h = \frac{p}{\rho_r g} + z = \psi + z \quad (6.4)$$

where ϕ is the porosity, S_w the saturation, S_s the specific storage, ψ the pressure head, K the unsaturated hydraulic conductivity, h the hydraulic head, t the time, z the height defined as positive upward, ρ_T the water density at the soil temperature T_s, ρ_r the reference water density at the reference soil temperature T_r, g the gravitational acceleration, β_s and β_w the compressibility coefficients of soil and water, respectively, K_r the relative hydraulic conductivity, K_T the correction-factor function of soil temperature, K_s the saturated hydraulic conductivity, S_e the effective saturation and p the water pressure.

6.2.2 Thermal transport model

The heat flux due to the water movement in soil is smaller than the heat conduction by the solid soil and thus can be neglected. Accordingly, the heat conduction equation assuming a local thermal equilibrium between soil and water is employed for the thermal transport, and described based on Kondo and Saigusa (1994)[33] as follows;

$$\frac{\partial (C_h T_s)}{\partial t} = -\frac{\partial}{\partial z}\left(-\lambda \frac{\partial T_s}{\partial z}\right) \quad (6.5)$$

with

$$C_h = (1-\phi)\,c_s + \theta c_w \quad (6.6)$$

$$\lambda = \lambda_0 + 0.5\theta^{\frac{1}{3}} \quad (6.7)$$

where C_h is the volumetric heat capacity of soil, θ the volumetric water content, c_s and c_w the volumetric heat capacity of soil particles (1.26×10^6 [J/(m^3·K)]) and that of water (4.20×10^6 [J/(m^3·K)]), respectively and λ the thermal conductivity of soil expressed in terms of the reference thermal conductivity λ_0 and volumetric water content.

6.2.3 Parameterization of soil hydraulic properties

Soil hydraulic properties to be identified are the unsaturated hydraulic conductivity and soil water retention curve.

The unsaturated hydraulic conductivity is described as the product of three variables shown in Eq.(6.3). The correction-factor function of soil temperature and saturated hydraulic conductivity are represented as follows.

$$K_{\mathrm{T}} = \frac{\mu_{\mathrm{r}}}{\mu_{\mathrm{T}}} \tag{6.8}$$

$$K_{\mathrm{s}} = \frac{\rho_{\mathrm{r}} g \varkappa}{\mu_{\mathrm{r}}} \tag{6.9}$$

where μ_{r} and μ_{T} are the dynamic viscosity coefficient at temperature T_{r} and T_{s}, respectively and $\varkappa$ the intrinsic permeability. Because the dynamic viscosity is the function of the temperature and the saturated hydraulic conductivity can be determined through laboratory experiments by definition, the parameterization of RHC is needed.

To represent RHC, a sequential piecewise cubic spline function is employed. This is referred to as a free-form approach indicating that no *a priori* shape of RHC is assumed except for their monotonicity (Bitterlich *et al*., 2004[3]). In the free-form approach, as shown in Figure 6.1, the effective saturation domain of interest is partitioned into $(I-1)$ subdomains with I nodes (I denotes the degrees of freedom of the parameterization), and the function for $K_{\mathrm{r}}(S_{\mathrm{e}})$ over whole domain $[S_{\mathrm{e}}(\theta_{\mathrm{r}}), S_{\mathrm{e}}(\theta_{\mathrm{s}})]$ is expressed by a summation of piecewise cubic spline interpolation functions which is locally defined over a confined subdomain bounded with two nodes. Thus, the function for $K_{\mathrm{r}}(S_{\mathrm{e}})$ with $K_{\mathrm{r},i}(S_{\mathrm{e}})$ defined over the ith subdomain $[S_{\mathrm{e},i}, S_{\mathrm{e},i+1}]$ is described as follows;

$$K_{\mathrm{r}}(S_{\mathrm{e}}) = \sum_{i=1}^{I-1} K_{\mathrm{r},i}(S_{\mathrm{e}}) \tag{6.10}$$

with

$$K_{\mathrm{r},i}(S_{\mathrm{e}}) = \begin{cases} a_i + b_i (S_{\mathrm{e}} - S_{\mathrm{e},i}) + c_i (S_{\mathrm{e}} - S_{\mathrm{e},i})^2 \\ \quad + d_i (S_{\mathrm{e}} - S_{\mathrm{e},i})^3, S_{\mathrm{e}} \in [S_{\mathrm{e},i}, S_{\mathrm{e},i+1}] \\ 0, \qquad\qquad S_{\mathrm{e}} \notin [S_{\mathrm{e},i}, S_{\mathrm{e},i+1}] \end{cases} \tag{6.11}$$

where a_i, b_i, c_i and d_i are coefficients in the cubic splines and i $(1 \le i \le I)$ a nodal number. Hereinafter, the values of $K_{\mathrm{r}}(S_{\mathrm{e}})$ at a node i are simply denoted by k_i. Since, as well known, RHC monotonously increases with the increasing saturation, Eq.(6.10) must be identified so that the following constraints are satisfied.

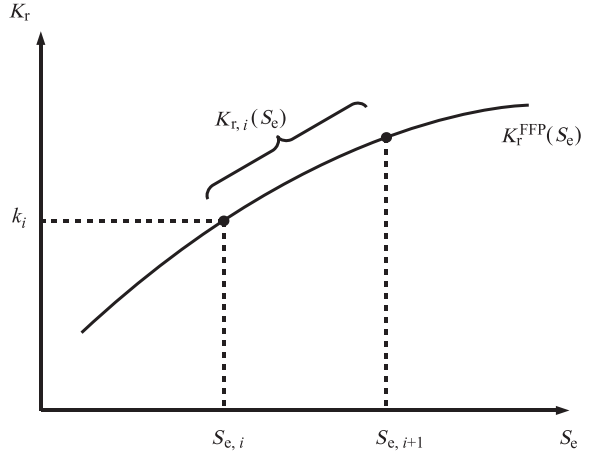

Figure 6.1: Free-form parameterization

$$k_i \le k_{i+1} \tag{6.12}$$

SWRC is a constitutive relation between the volumetric water content and pressure head. Various models have been proposed to represent SWRC. Among them, VG model has been more frequently used for the simulation of water movement in soil, and thus, VG model is employed for the representation of SWRC in this study. Additionally, to account for the effect of soil temperature when calculating θ using VG model, the value of ψ obtained from Eq.(6.1) is multiplied by two temperature correction coefficients. One is the ratio of the surface tensions at the soil temperature of interest and a reference temperature, and another is that of water density. This results in the following;

$$S_{\mathrm{e}}(\psi_{\mathrm{r}}) = \frac{1}{(1 + (\alpha_{\mathrm{vg}} |\psi_{\mathrm{r}}|)^{n_{\mathrm{vg}}})^{m_{\mathrm{vg}}}} = \frac{\theta - \theta_{\mathrm{r}}}{\theta_{\mathrm{s}} - \theta_{\mathrm{r}}} \tag{6.13}$$

with

$$m_{\mathrm{vg}} = 1 - \frac{1}{n_{\mathrm{vg}}} \tag{6.14}$$

$$\psi_{\mathrm{r}} = \frac{\sigma_{\mathrm{r}}}{\sigma_{\mathrm{T}}} \frac{\rho_{\mathrm{T}}}{\rho_{\mathrm{r}}} \psi \tag{6.15}$$

where θ_{r} is the residual water content, θ_{s} the saturated water content, α_{vg}, m_{vg} and n_{vg} the unknown parameters, ψ_{r} the pressure head at a reference soil temperature T_{r} and σ_{T} and σ_{r} the surface tension at soil temperature T_{s} and a reference temperature T_{r}, respectively.

6.2.4 Numerical solution procedure

After discretization with the combination of the standard Galerkin finite element method for space and the finite difference method for time, Eqs.(6.1) and (6.5) are subjected to the following initial and boundary conditions and numerically solved with the iterative partitioned method;

$$\psi(z, 0) = \psi_0(z) \qquad \text{in} \quad \Omega \tag{6.16}$$

$$T_{\mathrm{s}}(z, 0) = T_0(z) \qquad \text{in} \quad \Omega \tag{6.17}$$

$$\psi(z, t) = \overline{\psi}(z, t) \qquad \text{on} \quad \Gamma_{\mathrm{w}}^{\mathrm{D}} \tag{6.18}$$

$$T_{\mathrm{s}}(z, t) = \overline{T_{\mathrm{s}}}(z, t) \qquad \text{on} \quad \Gamma_{\mathrm{h}}^{\mathrm{D}} \tag{6.19}$$

$$-K_{\mathrm{s}} K_{\mathrm{r}} \frac{\partial h(z, t)}{\partial z} = \overline{q_{\mathrm{w}}}(z, t) \quad \text{on} \quad \Gamma_{\mathrm{w}}^{\mathrm{N}} \tag{6.20}$$

$$-\lambda \frac{\partial T_{\mathrm{s}}(z, t)}{\partial z} = \overline{q_{\mathrm{h}}}(z, t) \quad \text{on} \quad \Gamma_{\mathrm{h}}^{\mathrm{N}} \tag{6.21}$$

where $\psi_0(z)$ and $T_0(z)$ are the initial value of the pressure head and soil temperature, respectively, Ω the space domain, $\overline{\psi}(z, t)$ and $\overline{T_{\mathrm{s}}}(z, t)$ the values of the pressure head and soil temperature on the Dirichlet boundary, respectively, $\Gamma_{\mathrm{w}}^{\mathrm{D}}$ and $\Gamma_{\mathrm{h}}^{\mathrm{D}}$ the Dirichlet boundary for the water movement and heat transport, respectively, $\overline{q_{\mathrm{w}}}(z, t)$ and $\overline{q_{\mathrm{h}}}(z, t)$ the water and heat flux on Neumann boundary, respectively and $\Gamma_{\mathrm{w}}^{\mathrm{N}}$ and $\Gamma_{\mathrm{h}}^{\mathrm{N}}$ the

Neumann boundary for the water movement and heat transport, respectively.

6.3 Parameter Identification Procedure

The unknown parameters to be identified are the soil hydraulic properties, *i.e.*, RHC and SWRC, as described above. If the parameters can be determined with certainty in advance, they should be treated as known parameters because the number of identified parameters should be kept as small as possible. RHC, in general, cannot be determined by the direct measurement while SWRC can be obtained from the time-series data of the pressure head and volumetric water content with relative ease. Hence, RHC is treated as the unknown parameter and is identified with use of inverse technique.

6.3.1 Inverse problem

To solve IP is to optimally decide the unknown parameters, $\boldsymbol{k} = k_i,\ 1 \le i \le I$, which minimize the objective function defined as the total least squares error integrated over space and time between the solution of FP ($\psi^{\mathrm{com}}(\boldsymbol{k})$) and the observed data (ψ^{obs}), and thereby IP is defined as follows;

$$J(\boldsymbol{k}^{\mathrm{opt}}) = \min J(\boldsymbol{k}),\ \boldsymbol{k}^{\mathrm{opt}}, \boldsymbol{k} \in K_{\mathrm{ad}} \tag{6.22}$$

with

$$J(\boldsymbol{k}) = \frac{1}{2}\sum_{l=1}^{L}\{f_l(\boldsymbol{k})\}^2 \tag{6.23}$$

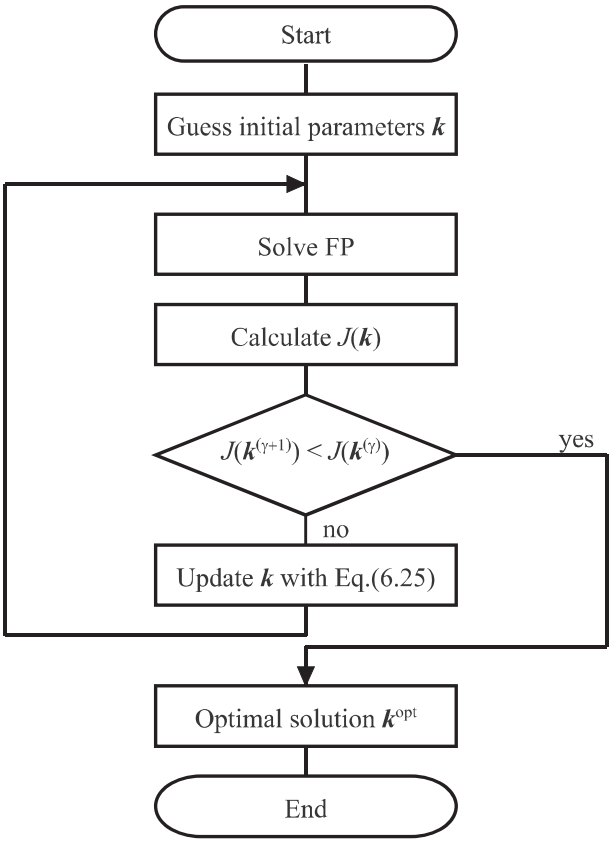

Figure 6.2: Flow chart for solving IP

$$f_l(\boldsymbol{k}) = w_l(\psi_l^{\mathrm{com}}(\boldsymbol{k}) - \psi_l^{\mathrm{obs}}) \tag{6.24}$$

where $\boldsymbol{k}^{\mathrm{opt}}$ is the set of optimal solutions, K_{ad} an admissible set of $\boldsymbol{k}^{\mathrm{opt}}$ and $\boldsymbol{k}$, L the total number of observed data available in space and time and w_l (normally, taken as unity) a weighting factor.

The process of solving IP is shown in Figure 6.2. The decision variables, $\boldsymbol{k}$, are iteratively modified or updated while step by step solving FP with their assumed or previously estimated values. In this respect, identification of RHC function (Eq.(6.10)) requires a sort of simulation-optimization technique.

6.3.2 Optimization algorithm

Levenberg-Marquardt method, which is a modified Gauss-Newton method combining the Gauss-Newton method and the gradient method, is employed for the optimization algorithm to search for the set of optimal solution with following search sequence through the iteration (Sun, 1994[51]);

$$\boldsymbol{k}^{(\gamma+1)} = \boldsymbol{k}^{(\gamma)} + \Delta\boldsymbol{k}^{(\gamma)} \tag{6.25}$$

with

$$\Delta\boldsymbol{k}^{(\gamma)} = -(\boldsymbol{H}^{(\gamma)} + \eta\boldsymbol{I})^{-1}\nabla J^{(\gamma)} \tag{6.26}$$

$$\boldsymbol{H}^{(\gamma)} = \left[\sum_{l=1}^{L}\frac{\partial f_l^{(\gamma)}}{\partial k_i}\frac{\partial f_l^{(\gamma)}}{\partial k_j}\right] \tag{6.27}$$

where γ is an iteration number, η a coefficient which controls search strategy between the Gauss-Newton and the steepest decent direction and $\boldsymbol{I}$ the $I \times I$ unit matrix.

6.4 Validation

Compared with the inverse modeling under isothermal assumption proposed by Izumi *et al*. (2010)[26], the applicability of this inverse modeling is assessed in terms of reproducibility for observed water movement in test soil. The time-series observed data is obtained through *in-situ* experiments (sandy soil) in Matsuyama, Ehime Prefecture.

6.4.1 Field observation and computational domain

The observation system and computational domain for parameter identification are illustrated in Figure 6.3.

The observation system consists of three sets of instruments—tensiometer (UIZ-SMT), soil moisture probe (UIZ-SM-2X) and thermometer (TMC20-HD)—and automatically records time-series data of the pressure head, volumetric water content and soil temperature at intervals of 10 minutes. To reduce the influence of direct solar radiation on the observed pressure heads, the sensors of tensiometers attached above ground are shielded by white-colored box with slits for ventilating air. Each set of instruments is buried at three different depths in a soil column: -10 cm, -20 cm and -30 cm. A pair of pressure head and volumetric water content data at the same depth is used to determine SWRC. The observed values of the pressure head at -20 cm deep is used to determine the

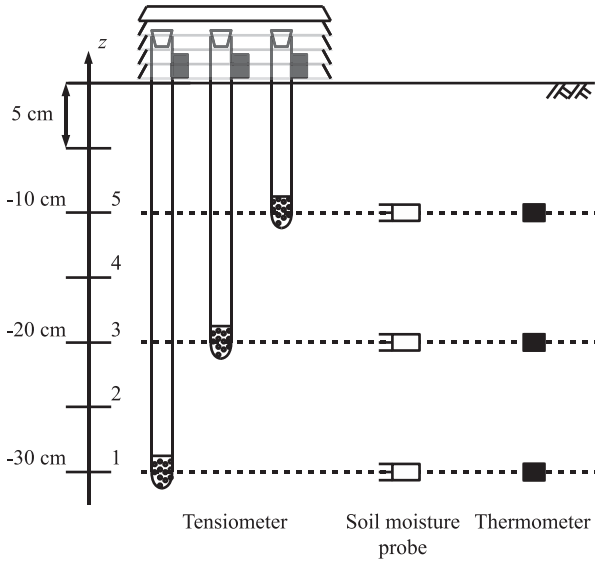

Figure 6.3: Schematic illustration of observation and computation

function shape of RHC (Eq.(6.10)) and to assess the fitness of estimated RHC function in the simulation-optimization runs. The pressure head and soil temperature observed at both top and bottom (-10 cm and -30 cm deep) of test soil are utilized as Dirichlet boundary values for solving FP to intentionally avoid measuring flux like evapotranspiration whose measurement is generally difficult in the field experiments. The time-series soil temperatures at -20 cm deep are used as the benchmark data for confirming reproducibility of forward solution.

The computational domain therefore is the surface soil of 20 cm thick between -10 cm and -30 cm deep, where the saturation and soil temperature vary significantly with meteorological conditions, and is divided into four equal elements with five nodes for numerical computations.

Like in most earlier works on parameter identification, a one-way process of desorption is considered for estimation of the soil hydraulic properties to exclude the hysteric phenomenon in this study. Hence, the data series observed during no-rainfall or desorption period—November 25 to December 2, 2010—and used for parameter identification and validation of the inverse modeling, is shown in Figure 6.4.

6.4.2 Identification of SWRC

SWRC is defined as the approximate curve for the scatter plots relating volumetric water content to pressure head, and should be determined before estimating RHC. To obtain θ-ψ relations at a reference soil temperature expressed by Eq.(6.13), van Genuchten *et al*. (1991)[60] proposed the RETC program which is an estimation method for unknown parameters included in SWRC function with use of the nonlinear least-squares approach. Generally, it is very important to input an adequate estimate of the initial value of unknown parameters for such nonlinear fitting. Since the RETC program does not have the function of automatically estimating the initial parameters, Seki (2007)[49] developed the alterative algorithm called SWRC fit. This nonlinear fitting software not only can automatically determine the initial estimate of unknown parameters, but also can accomplish the parameter identification for the five SWRC models including VG model. Accordingly, SWRC fit is employed to identify the reference θ-ψ relations.

For the implementation, observed data of θ and ψ are corrected for a reference temperature based on the soil temperature observed at the same depth, using the coefficient of thermal expansion and Eq.(6.15), respectively. Additionally, the saturated water content θ_s is defined as the value of θ in case that ψ is equal to zero while the residual water content θ_r as the minimum value in all observed data of θ. Thus, θ_s and θ_r are determined to be 0.30 and 0.05 from all observed data series including them shown in Figure 6.4, respectively. As the reference soil temperature, the average value of observed data is adopted which equals to 12.4 degrees Celsius.

Conclusively, a best fitting curve for θ-ψ relation at the reference soil temperature is obtained with the value of α_{vg} and n_{vg} being 28.9 m^{-1} and 1.43, respectively, as shown in Figure 6.5.

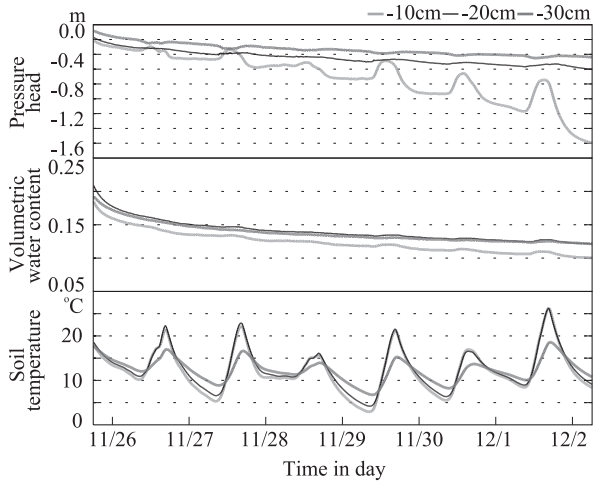

Figure 6.4: Observed data

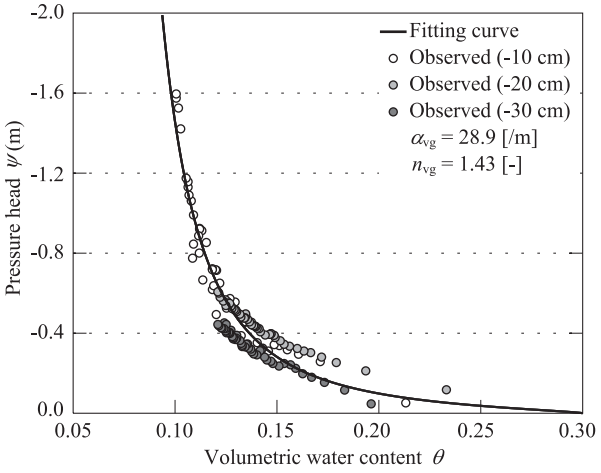

Figure 6.5: Identified SWRC

6.4.3 Identification of RHC

Firstly, the number of identified unknown parameters is determined. In the free form approach, the large number of parameters can be set for the functional form of RHC to have high flexibility or degree of freedom. However, the large number of parameters cause the increasing uncertainty of identified parameters, making IP difficult to solve. For this, the identified parameter number should be kept to the minimum in general. Since the optimal number of parameters is approximately from seven to nine according to Bitterlich *et al*. (2004)[3] and Iden and Durner (2007)[21], the number of unknown parameters is set to be 10.

Secondly, the manner of division on the definition domain—effective saturation domain—is determined. The functional shape of RHC generally has steeper gradient near the saturated zone. In the context of accuracy, the range with steeper gradient should be divided into finer subdomain. Therefore the effective saturation range from 0.8 to 1.0 where RHC function rapidly changes is partitioned into sub-range in the manner of geometric series.

Eventually, RHC function is identified as shown in Figure 6.6 after the saturated hydraulic conductivity at the reference temperature is determined to be 5.18×10^{-5} m/s through laboratory experiment.

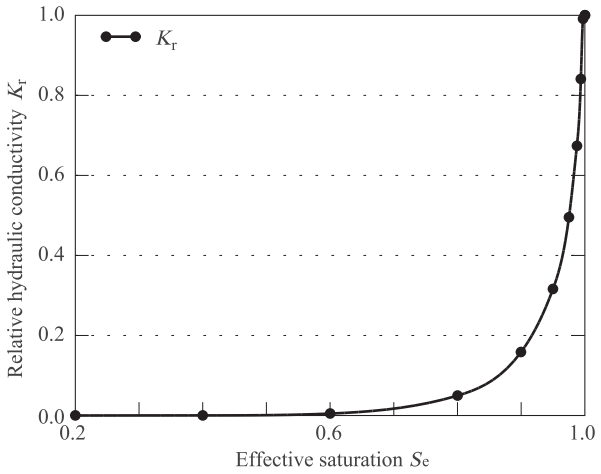

Figure 6.6: Identified RHC

6.4.4 Reproducibility of calibrated forward simulation model for variably saturated subsurface flow

The applicability of the inverse modeling presently developed is assessed in terms of reproducibility for the time-series observed data by calibrated forward simulation model through comparing the observed and computed values. The result of reproducibility for water movement and heat transport are shown in Figures 6.7 and 6.8, respectively. In the lower half of Figure 6.7, the absolute errors $|\psi^{\mathrm{com}} - \psi^{\mathrm{obs}}|$ are also shown to demonstrate the time-varying difference in solution reproducibility. From the result, it is found that both water movement and heat

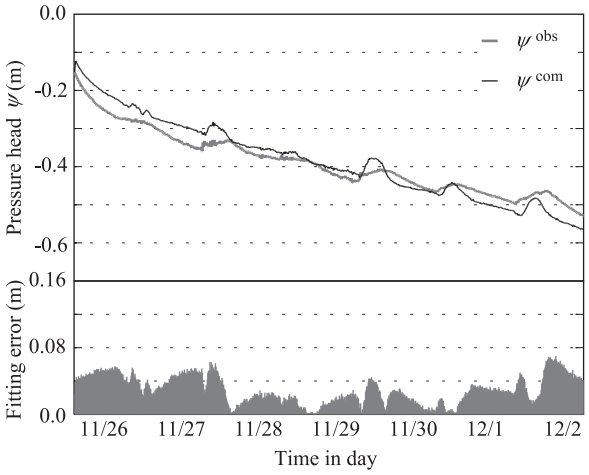

Figure 6.7: Reproducibility of forward solution for water movement

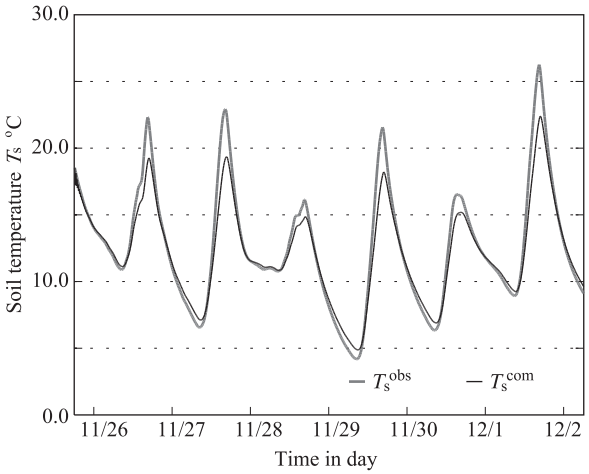

Figure 6.8: Reproducibility of forward solution for heat transport

transport are reproduced with high accuracy.

For the purpose of comparison, the preceding inverse modeling proposed by Izumi *et al*. (2010)[26], which did not consider the influence of soil temperature on water movement, is applied to the same observed data. In Figures 6.9 and 6.10, the results for identification of RHC and the reproducibility of forward solution for water movement are shown in a similar trend of Figures 6.6 and 6.7, respectively. Hereinafter, the proposed model in this chapter is referred to as the non-isothermal model and the model proposed by Izumi *et al*. (2010)[26] is referred to as the isothermal model. In addition, the values of the objective function $J(\boldsymbol{k})$ for both models are summarized in Table 6.1 to supply superiority of the non-isothermal model with a quantitative underpinning. The comparison results indicate that consideration of temperature-dependency is beneficial to simulate the water flow near the soil surface, and thus it concludes that the inverse model proposed provide a high performance for the modeling of subsurface water flow.

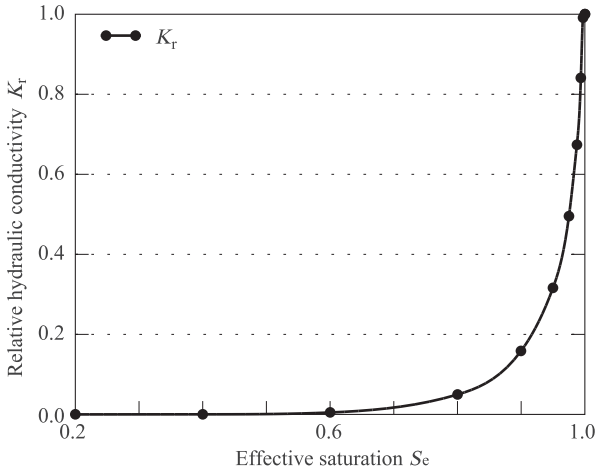

Figure 6.9: Identified RHC by isothermal model

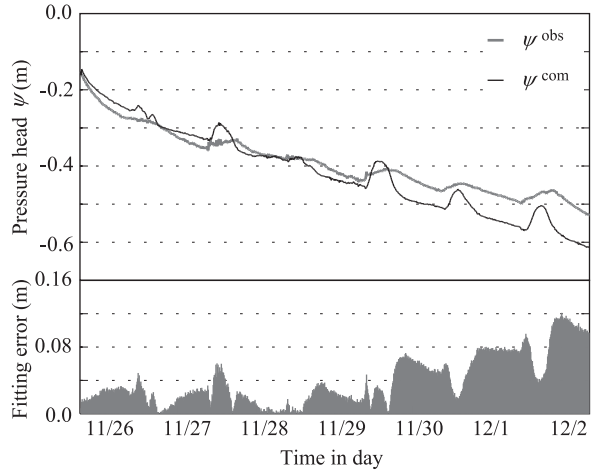

Figure 6.10: Reproducibility of forward solution for water movement in isothermal model

Table 6.1: Optimal values of $J(\boldsymbol{k})$

Model	$J(\boldsymbol{k})$
Non-isothermal model	1.091
Isothermal model	2.362

6.5 Conclusions

An inverse modeling for variably saturated and non-isothermal subsurface water flow is developed. To consider the water movement depending on the soil temperature, a couple of mixed form of Richards equation with heat conduction equation is employed as the governing equation which describes the forward problem. The soil hydraulic properties which are the model parameters included in the governing equation are the soil water retention curve and unsaturated (or relative) hydraulic conductivity. Since the former is determined through experiments with relative ease, the latter is unknown parameter in this study. For the functional form of the relative hydraulic conductivity, the free-form approach is employed. The inverse problem to identify the relative hydraulic conductivity function is defined and solved for the practical field experiments with *in-situ* soil column near the surface soil to evaluate the performance of proposed method. From the examination and comparison of the preceding method which did not consider the influence of soil temperature on the water movement, the advantage and appropriateness of this method is shown and the importance of consideration for the temperature-dependency in the water movement near the soil surface is emphasized.

CHAPTER 7

SUMMARY AND CONCLUSIONS

In this thesis, inverse modeling of variably saturated subsurface water flow in isothermal/non-isothermal soil is studied, considering the following three forms of Richards equation which describe subsurface water flow.

(1) ψ-based form Richards equation

(2) θ-based form Richards equation

(3) Mixed form Richards equation

In Chapter 3, an inverse method to identify a function form of the soil hydraulic properties, *i.e.*, the water retention curve and unsaturated hydraulic conductivity, in variably saturated subsurface water flow model described as the ψ-based form Richards equation is developed. The soil hydraulic properties are represented by a free form function composed of sequential piecewise cubic spline functions. The functions are used as an alternative to the conventional fixed form functions in order to increase accuracy of forward problems (numerical analyses or simulations). The inverse problem is formulated into the optimization problem minimizing the objective function. The objective function is defined as the total squared error integrated over space and time between the computed and observed pressure head, which is the decision variable in the ψ-based form Richards equation. It is then solved by a simulation-optimization algorithm with the aid of the Levenberg-Marquardt method. Validity of the method is examined through twin experiments applying it to two different soil types which are representative to the sensitivity of the relative hydraulic conductivity near saturation. The results show that the soil hydraulic properties could be successfully identified with a free form function, and therefore, the approach could be a viable alternative to the conventional fixed form function approaches.

In Chapter 4, an inverse method to identify the unsaturated hydraulic conductivity in variably saturated subsurface water flow model in non-isothermal soil described as coupled equation of the θ-based form Richards equation and heat conduction equation is proposed. An *in-situ* observation with simple instrumentation set-up collects the hydro-geological data necessary in solving the inverse problem. For the parameterization of the soil hydraulic properties, a free form function formed by sequential piecewise cubic spline functions is used for the unsaturated hydraulic conductivity and van Genuchten model is used for the soil water retention curve. Using the same manner as that described in Chapter 3, an inverse problem is defined for the objective function in terms of the decision variable θ in the θ-based form Richards equation which is used to describe the forward problem for water movement. The validity confirmation is carried out by applying the method to three serial data during desorption in field soil. From the results, the following issues are concluded:

(1) the relative hydraulic conductivity could be successfully identified by a free form function

(2) the present approach of reflecting the effect of thermal conduction on water movement and employing the free form parameterization technique could be a practical alternative to the conventional approaches, and

(3) the specially-contrived and inexpensive observation system enriches utility of the approach.

In Chapter 5, an inverse method to identify the unsaturated hydraulic conductivity in variably saturated subsurface water flow model described as the mixed form Richards equation is proposed. As the basic equation governing the forward problem, the mixed form Richards equation is considered which is conservative in terms of mass balance. The unsaturated hydraulic conductivity, the model parameter to be identified in the mixed form Richards equation, is represented by a free form function composed of sequential piecewise cubic spline functions. An inverse problem to determine the function form of the unsaturated hydraulic conductivity is defined as the optimization problem to minimize errors between the observed and computed pressure heads, and solved with the use of a simulation-optimization technique. The developed method is applied to an *in-situ* soil column and its validity is examined in terms of reproducibility of desorption process in the soil. The results indicate that a coupled model of water movement and heat transport should be considered.

In Chapter 6, an inverse method to identify the unsaturated hydraulic conductivity in variably saturated subsurface water flow model in non-isothermal soil described as coupled equation of the mixed form Richards equation and heat conduction equation is discussed. The present method is an extension of the method presented in Chapter 5 to consider water movement in surface soil depending on soil temperature, and thus, is developed using the same method, except for the governing equation. Validity of the method is tested and confirmed through practical application to an *in-situ* soil column and through comparison with the previous method.

ACKNOWLEDGMENTS

The author would like to express his sincerest appreciation and deepest gratitude to Dr. Toshihiko KAWACHI, Professor of Water Resources Engineering, Division of Environmental Science and Technology, Graduate School of Agriculture, Kyoto University, and Chairperson of the Dissertation Committee, for his keen guidance, valuable suggestions, constructive criticisms, continuous support and encouragement in the completion of this dissertation. Author's gratitude to him cannot be fully acknowledged here.

The author would also like to extend his sincere appreciation to the members of his Dissertation Committee: Professor Dr. Akira MURAKAMI and Professor Dr. Shigeto KAWASHIMA, for their valuable discussions and advice in reviewing and improving this thesis.

The author wishes to express special thanks to Dr. Masayuki FUJIHARA, Professor of Water Resources Engineering, Department of Rural Engineering, Faculty of Agriculture, Ehime University, and Dr. Junichiro TAKEUCHI, Instructor of Water Resources Engineering, Division of Environmental Science and Technology, Graduate School of Agriculture, Kyoto University, for their warm support, valuable comments and technical assistance over the research period.

Heartfelt thanks are also due to Associate Professor Dr. Koichi UNAMI and Lecturer Dr. Shigeya MAEDA of Water Resources Engineering, Division of Environmental Science and Technology, Graduate School of Agriculture, Kyoto University, for their fruitful comments and technical assistance.

The author would also like to express his appreciation to the researchers and professors of the Department of Rural Engineering, Faculty of Agriculture, Ehime University, and Associate Professor Dr. Kunihiko HAMAGAMI of Iwate University, for their hearty support, cooperation and useful recommendation.

The author also likes to thank all members of Water Resources Engineering Laboratory of both Ehime and Kyoto University, the former and current students and Ms. Masumi HASHIMOTO, secretary of the Laboratory of Kyoto University, for their assistance, cooperation and inspiration in all respects of the study period.

The author is grateful to his family for their wholehearted support and is dedicating this thesis to his parents, Akihiro and Keiko. Finally, the author also likes to thank "Aizen-myoo", the principal Buddhist statue in Kongoshin-in Temple, and Kobo Daishi, for their protection.

REFERENCES

[1] Akai, K., Y. Ohnishi and M. Nishigaki ; Finite element analysis of saturated-unsaturated seepage in soil, *Proceedings of the Japan Society of Civil Engineers*, (264), pp. 87－96, 1973 (in Japanese)

[2] Allen, R. G., L. S. Pereira, D. Raes and M. Smith ; Crop evapotranspiration: Guidelines for computing crop water requirements, *Irrigation and Drainage Paper*, (56), FAO, Rome, 300p 1998

[3] Bitterlich, S., W. Durner, S. C. Iden and P. Knabner ; Inverse estimation of the unsaturated soil hydraulic properties from column outflow experiments using free-form parameterizations, *Vadose Zone Journal*, 3(3), pp. 971－981, 2004

[4] Broadbridge, P. and I. White ; Constant rate rainfall infiltration: a versatile nonlinear model. 1. analytic solution, *Water Resources Research*, 24(1), pp. 145－154, 1988

[5] Brooks, R. H. and A. T. Corey ; Properties of porous media affecting fluid flow, *Journal of the Irrigation and Drainage Division, Proceedings of the American Society of Civil Engineers*, 92(IR2), pp. 61－88, 1966

[6] Celia, M. A., E. T. Bouloutas and R. L. Zarba ; A general mass-conservative numerical solution for the unsaturated flow equation, *Water Resources Research*, 26(7), pp. 1483－1496, 1990

[7] Cohen, J. E. ; *How Many People Can the Earth Support?*, Norton, 532p, 1995

[8] Constales, D. and J. Kačur ; Determination of soil parameters via the solution of inverse problems in infiltration, *Computational Geosciences*, 5(1), pp. 25－46, 2001

[9] de Vries, D. A. ; Simultaneous transfer of heat and moisture in porous media, *Transactions of American Geophysical Union*, 39(5), pp. 909－916, 1958

[10] Durner, W. ; Hydraulic conductivity estimation for soils with heterogeneous pore structure, *Water Resources Research*, 30(2), pp. 211－223, 1994

[11] Eching, S. O. and J. W. Hopmans ; Optimization of hydraulic functions from transient outflow and soil water pressure data, *Soil Science Society of America Journal*, 57(5), pp. 1167－1175, 1993

[12] Falkenmark, M., J. Lundqvist and C. Widstrand ; Macro-scale water scarcity requires micro-scale approaches, *Natural Resources Forum*, 13(4), pp. 258－267, 1989

[13] FOA ; AQUASTAT Online Database, 2011 http://www.fao.org/nr/water/aquastat/main/index.stm

[14] Fujinawa, K. ; Coupled analysis of heat transport and water flow with hysteresis in saturated-unsaturated porous media, *Journal of Groundwater Hydrology*, 37(3), pp. 175－192, 1995 (in Japanese)

[15] Fujinawa, K. ; *Environmental Groundwater Science*, Kyoritsu Publishing, 354p, 2010 (in Japanese)

[16] Hillel, D. ; *Environmental Soil Physics*, Academic Press, 771p, 1998

[17] Hills, R. G., I. Porro, D. B. Hudson and P. J. Wierenga ; Modeling one-dimensional infiltration into very dry soils: 1. Model development and evaluation, *Water Resources Research*, 25(6), pp. 1259－1269, 1989

[18] Hsu, R. and C.L. Liu ; Use of parameter estimation in determining soil hydraulic properties from unsaturated

transient flow, *Water Resources Management*, 4(1), pp. 1－19, 1990

[19] Huang, K., B. P. Mohanty and M. Th. van Genuchten ; A new convergence criterion for the modified picard iteration method to solve the variably saturated flow equation, *Journal of Hydrology*, 178(1－4), pp. 69－91, 1996

[20] Huyakorn, P. S. and G. F. Pinder ; *Computational Methods in Subsurface Flow*, Academic Press, 473p, 1983

[21] Iden, S. C. and W. Durner ; Free-form estimation of the unsaturated soil hydraulic properties by inverse modeling using global optimization, *Water Resources Research*, 43(7), W07451, 2007

[22] Iden, S.C. andW. Durner ; Free-form estimation of soil hydraulic properties using Wind's method, *European Journal of Soil Science*, 59(6), pp. 1228－1240, 2008

[23] Inoue, M., T. Morii, T. Nishimura and H. Fujimaki ; In-situ determination of unsaturated hydraulic conductivity using profile probe, *Transactions of the Japanese Society Irrigation, Drainage and Rural Enginnering*, (231), pp. 39－45, 2004 (in Japanese)

[24] IPCC ; *Climate Change 2007: Synthesis Report*, Contribution ofWorking Groups I, II and III to the Fourth Assessment Report of the Intergovernmental Panel on Climate Change, 104p, 2007

[25] Ippisch, O., H. J. Vogel and P. Bastian ; Validity limits for the van Genuchten-Mualem model and implications for parameter estimation and numerical simulation, *Advances in Water Resources*, 29(12), pp. 1780－1789, 2006

[26] Izumi, T., M. Fujihara, J. Takeuchi and T. Kawachi ; Inverse modeling of massconservative numerical model for variably saturated seepage flow, *Journal of Rainwater Catchment Systems*, 17(1), pp. 11－16, 2011

[27] Izumi, T., J. Takeuchi, T. Kawachi and M. Fujihara ; An inverse method to estimate unsaturated hydraulic conductivity in seepage flow in non-isothermal soil, *Transactions of the Japanese Society Irrigation, Drainage and Rural Enginnering*, (264), pp. 35－42, 2009

[28] Izumi, T., J. Takeuchi, T. Kawachi, K. Unami and S. Maeda ; An inverse method to estimate soil hydraulic properties in saturated-unsaturated groundwater flow model, *Journal of Rainwater Catchment Systems*, 13(2), pp. 23－28, 2008

[29] Japanese Association of Groundwater Hydrology ; *Simulation of Groundwater Flow and Solute Transport*, Gihodo Publishing, 232p, 2010 (in Japanese)

[30] Jury, W.A. and R. Horton ; *Soil Physics*, John Wiley & Sons, 370p, 2004

[31] Kastanek, F. J. and D. R. Nielsen ; Description of soil water characteristics using cubic spline interpolation, *Soil Science Society of America Journal*, 65(2), pp. 279－283, 2001

[32] Klute, A. ; A numerical method for solving the flow equation for water in unsaturated materials, *Soil Science*, 73(2), pp. 105－116, 1952

[33] Kondo, J. and N. Saigusa ; Modeling the evaporation from bare soil with a formula for vaporization in the soil pores, *Journal of Meteorological Society of Japan*, 72, pp. 413－421, 1994 (in Japanese)

[34] Kosugi, K. ; Three-parameter lognormal distribution model for soil water retention, *Water Resources Research*, 30(4), pp. 879－890, 1994

[35] Kosugi, K. ; Lognormal distribution model for unsaturated soil hydraulic properties, *Water Resources Research*, 32(9), pp. 2697－2703, 1996

[36] Milly, P. C. D. ; Moisture and heat transport in hysteretic, inhomogeneous porous media: A matric head-based formulation and a numerical model, *Water Resources Research*, 18(3), pp. 489－498, 1982

[37] Milly, P. C. D. ; A similation analysis of thermal effects on evaporation from soil, *Water Resources Research*, 20(8), pp. 1087－1098, 1984

[38] Milly, P. C. D. ; A mass-conservative procedure for time-stepping in models of unsaturated flow, *Advances in Water Resources*, 8(3), pp. 32－36, 1985

[39] Ministry of Land, Infrastructure, Transport and Tourism ; *Water Resources in Japan*, 209p, 2011 (in Japanese)

[40] Ministry of the Environment ; *2010 Annual Report on the Environment, the Sound Material-cycle Society and the Biodiversity in Japan: Our Responsibility and Commitment to Preserve the Earth －Challenge 25－*, 169p, 2011

[41] Moukalled, F. and Y. Saleh ; Heat and mass transport in moist soil, part I. formulation and testing, *Numerical Heat Transfer, Part B*, 49, pp. 467－486, 2006

[42] Mualem, Y. ; New model for predicting the hydraulic conductivity of unsaturated porous media, *Water Resources Research*, 12(3), pp. 513－522, 1976

[43] Neuman, S. P. ; Saturated-unsaturated seepage by finite elements, *Journal of the Hydraulics Division, Proceedings of the American Society of Civil Engineers*, 99(HY12), pp. 2233－2250, 1973

[44] Neuman, S. P. and P. A. Witherspoon ; Finite element method of analyzing steady seepage with a free surface, *Water Resources Research*, 6(3), pp. 889－897, 1970

[45] Neuman, S. P. and P. A. Witherspoon ; Analysis of nonsteady flow with a free surface using the finite element method, *Water Resources Research*, 7(3), pp. 611－623, 1971

[46] Philip, J. R. and D. A. de Vries ; Moisture movement in porous materials under temperature gradients, *Transactions of American Geophysical Union*, 38(2), pp. 222－232, 1957

[47] Richards, L. A. ; Capillary conduction of liquids through porous mediums, *Journal of Applied Physics*, 1(5), pp. 318－333, 1931

[48] Scanlon, B. R. and P. C. D. Milly ; Water and heat fluxes in desert soils: 2. Numerical simulations, *Water Resources Research*, 30(3), pp. 721－733, 1994

[49] Seki, K. ; SWRC fit －A nonlinear fitting program with a water retention curve for soils having unimodal and bimodal pore structure, *Hydrology and Earth System Sciences Discussions*, 4(1), pp. 407－437, 2007

[50] Si, B.C. and R.G. Kachanoski ; Estimating soil hydraulic properties during constant flux infiltration: Inverse procedures, *Soil Science Society of America Journal*, 64(2), pp. 439－449, 2000

[51] Sun, N. Z. ; *Inverse Problems in Groundwater Modeling*, Kluwer Academic Publishers, 337p, 1994

[52] Takeshita, Y. and I. Kohno ; A method to pedict

hydraulic properties for unsaturated soils and its application to observed data, *Ground Engineering; Journal of Chugoku Branch, JGS*, 11(1), pp. 95－113, 1993 (in Japanese)
[53] Takeuchi, J., T. Izumi and T. Kawachi ; An inverse method for unsaturated hydraulic conductivity based on in-situ observation, *Proceedings of the 15th Annual Congress of Japan Rainwater Catchment Systems Association*, 15, pp. 5－8, 2007 (in Japanese)
[54] Takeuchi, J., T. Kawachi and T. Izumi ; Explicit scheme for mixed form of Richards equation, *Proceedings of the Japanese Society of Irrigation, Drainage and Rural Engineering*, pp. 322－323, 2008 (in Japanese)
[55] United Nations Development Programme (UNDP) ; *Human Development Report 2006: Beyond scarcity; power, poverty and the global water crisis*, 422p, 2006
[56] United Nations Population Division ; *World Population Prospects: the 2010 Revision*, 2010 http://esa.un.org/unpd/wpp/index.htm
[57] Šimůnek, J., O. Wendroth and M. Th. van Genuchten ; Parameter estimation analysis of the evaporation method for determining soil hydraulic properties, *Soil Science Society of America Journal*, 62(4), pp. 894－905, 1998
[58] van Dam, J. C., J. N. M. Stricker and P. Droogers ; Inverse method to determine soil hydraulic functions from multistep outflow experiments, *Soil Science Society of America Journal*, 58(3), pp. 647－652, 1994
[59] van Genuchten, M. Th. ; A closed-form equation for predicting the hydraulic conductivity of unsaturated soils, *Soil Science Society of America Journal*, 44(5), pp. 892－898, 1980
[60] van Genuchten, M. Th., F. J. Leij and S. R. Yates ; *The RETC code for quantifying the hydraulic functions of unsaturated soils*, Technical Report EPA/600/2-91/065, US Environmental Protection Agency, 85p, 1991
[61] Vogel, T., M. Th. van Genuchten and M. Cislerova ; Effect of the shape of the soil hydraulic functions near saturation on variably-saturated flow predictions, *Advances in Water Resources*, 24(2), pp. 133－144, 2001
[62] Zadeh, K. S. ; A mass-conservative switching algorithm for modeling fluid flow in variably saturated porous media, *Journal of Computational Physics*, 230(3), pp. 664－679, 2011
[63] Zhang, K., I. G. Burns, D. J. Greenwood, J. P. Hammond and P. J. White ; Developing a reliable strategy to infer the effective soil hydraulic properties from field evaporation experiments for agro-hydrological models, *AgriculturalWater Management*, 97(3), pp. 399－409, 2010
[64] Zienkiewicz, O. C., P. Mayer and Y. K. Cheung ; Solution of anisotropic seepage by finite elements, *Journal of the Engineering Mechanics Division, Proceedings of the American Society of Civil Engineers*, 92(EM1), pp. 111－120, 1966